NMR STUDIES OF SOME LITHIUM BASED FAST ION CONDUCTORS

Mohamed Tawfik El-Gamal, M.Sc.

A thesis submitted to the University of Warwick for admission to the degree of Doctor of Philosophy

Department of Physics

February 1988

To my wife Najjat and my children Hisham, Hitham and Halilima

ACKNOWLEDGEMENTS

DECLARATION

ABSTRACT

ACKNOWLEDGEMENTS

I would like to thank my supervisor, Dr. R. Dupree, for his interest, help and involvement during this study. Also I am grateful to Dr. I. Farnan, Dr. M.E. Smith and Mr. G. Mortuza for many valuable discussions. The practical assistance of Mr. B. Sheffield and Mr. K. Briggs is really appreciated. I am grateful to the Ministry of Education, Libya for the financial support.

Finally, I would like to thank Mrs. C. Gow for her accurate and speedy typing.

DECLARATION

This thesis is submitted to the University of Warwick in support of my application for admission to the Degree of Doctor of Philosophy. It contains the work carried out under the supervision of Dr. R. Dupree, during the period of November 1983 to February 1988. No part of this work has appeared in any thesis at this or any other institution. The work reported in this thesis is the result of my own independent research except where specifically acknowledged.

M.T. EL-GEMAL

ABSTRACT

The spin lattice and spin-spin relaxation times T_1 and T_2 when measured as a function of temperature and frequency provide information about the activation energies and the correlation times which help in understanding the conduction mechanism in fast ion conductors. Dilithium trititanate $Li_2Ti_3O_7$ according to data reported by Huberman and Boyce shows an unusual frequency dependent T_1 and an anomalously low value of attempt frequency of 4×10^7 Hz. was deduced. The activation energy from the motional narrowing region of T_2 was 0.2 eV compared with 0.45 eV from the conductivity measurements. Various explanations were put forward to justify these anomalies including "the break-down of the absolute rate theory" and also Richards put forward a theory to account for these discrepancies assuming that the conduction in these channel type materials is one dimensional. T_1 and T_2 have been measured for ^7Li in very pure, highly stoichiometric material and off-stoichiometric material at different temperatures and at several frequencies. The value of T_1 and T_2 obtained for the stoichiometric sample is more than an order of magnitude longer than those observed by Huberman and Boyce over most of the temperature range and the activation energy obtained from the motional narrowing region of T_2 is very close to that obtained from the conductivity. Also the attempt frequency found through T_1 minimum is more than two orders of magnitude higher than the reported value of Huberman and Boyce. Small departures from stoichiometry rapidly reduce the relaxation times. The results are discussed in terms of the presence of paramagnetic ions in this material.

Some of the lisicon group such as $Li_{12}Mg_2(SiO_4)_4$ and $Li_{12}Zn_2(SiO_4)_4$ are also investigated through measurements of T_1 and T_2 in the temperature

range between 150°C and 400°C. The activation energies obtained from T_1 and the motional narrowing region of T_2 are the same with values of 0.5 eV and 0.43 eV and attempt frequencies of 1×10^{12} Hz. and 0.47×10^{12} Hz. for $Li_{12}Mg_2(SiO_4)_4$ and $Li_{12}Zn_2(SiO_4)_4$ respectively. Below the minimum T_1 varies with the frequency as $\omega^{1.5}$. The results are also discussed in terms of the presence of paramagnetic ions in the materials.

CHAPTER ONE

FAST ION CONDUCTORS

1.1 Introduction

Ionic solids have been used as solid electrolytes for many years. They have been investigated from many different points of view yielding valuable information about their transport properties. In these materials, the transport phenomena are governed by the displacement of ions (Lidiard (1957)). The ionic conductivity of most ionic solids is very low at temperatures well below their melting points, usually less than 10^{-10} $(\Omega\ cm)^{-1}$ at room temperature.

During the last two decades a number of very good ionic conductors with high ionic conductivity at room temperature have been discovered. They have received a good deal of attention. There are a number of recent review articles by Widerisch and Geller (1970), Takahashi (1973), Van Gool (1973) and Boyce (1977) and a number of books by Chandra (1981), Hagenmuller (1978), and conference proceedings Bates (1981) and Kleitz (1983), relating to the study of these ionic conductors. They are ionic but exhibit various special features.

(i) The magnitude of conductivity is very large 10^{-1} - 10^{-4} $(\Omega\ cm)^{-1}$ at room temperature, compared with conventional ionic solids, and is insensitive to impurities. For example the ionic conductivity of Ag_4RbI_5, which is a fast ion conductor above a temperature of 250K is about 17 orders of magnitude larger than that of NaCl at the same temperature (Dreyfus, R.W. et al 1962).

(ii) The conductivity is far less dependent on temperature than the conventional ionic solids. This is due to the existence of large

number of defect sites which allow the ions to hop around.

(iii) The activation energy is of the order of 0.1-0.5 ev while for conventional solids it is about 1-3 ev.

(iv) The electronic conductivity is negligibly small about 10^{-8} $(\Omega\ cm)^{-1}$. This property is important particularly in the field of solid state batteries.

The electrical conductivity of some fast ion conductors (FIC) versus inverse temperature is shown in fig. (1.1). Ag_4RbI_5 which has the highest ionic conductivity at 250K and was first discovered in the silver ion conducting group has triggered an active field where different researchers from different fields of science have been trying to discover materials with ever higher conductivity. These new compounds, due to their high ionic conductivity have become of great importance in technology, for example in the solid state batteries, pace makers, etc. A good classification is based on the type of phase transformation exhibited by different solids. This has led to three types of fast ion conductor behaviour as shown in fig. (1.2).

(i) A first order phase change as in the case of AgI where $\beta \rightarrow \alpha$ transformation occurs at a temperature of 147°C and increases the conductivity by four orders of magnitude.

(ii) A gradual transition from insulating to conducting state. This transition results in a rapid increase of conductivity with temperature and a relatively small activation energy. This behaviour is shown in the case of PbF_2.

(iii) An exponential growth in ionic conductivity as the temperature is increased without showing any phase change as in the cases of Na β-alumina and $Li_2Ti_3O_7$.

The high ionic conductivity in these solids is attributed to some

type of disorder. In the case of α AgI which represents a large group of fast ion conductors, an x-ray investigation by Strock (1934) concluded that for the two silver ions in the unit cell there are forty two sites available for conduction. Geller (1972) studied the structure of most AgI based fast ion conductors and found that Ag^+ ions in all of them are highly disordered and distributed statistically over a large number of sites. At room temperature AgI has a hexagonal structure referred to as βAgI. At temperature of 147°C a phase change occurs transforming to α AgI which has a body centred cubic structure with I^- ions making the rigid structure of BCC. The ionic conductivity below 147°C is 3×10^{-2} $(\Omega\ cm)^{-1}$, it increases abruptly at 147°C to 1.3×10^{2} $(\Omega\ cm)^{-1}$ and does not appreciably alter after that temperature.

Another important class of fast ion conductors known as β-alumina has been studied extensively by Kennedy (1977). These solids have the general formula

$$A_2O \cdot nM_2O_3$$

where A = Na, Rb, Ag, K, Li

M = Aℓ, Ga

and n = 5-11 (integer)

The crystal structure is basically hexagonal and shows layered formation perpendicular to the c-direction. Blocks of aluminium and oxygen ions provide the main structure. Between these blocks there is a bridge layer in which the ions such as Na^+ responsible for conductivity resides. The amount of sodium ions in this layer varies resulting in a structure which provides the Na^+ ions with more sites than the equivalent ions.

1.2 Ionic Conductivity

Defects are known to be thermally generated in conventional ionic

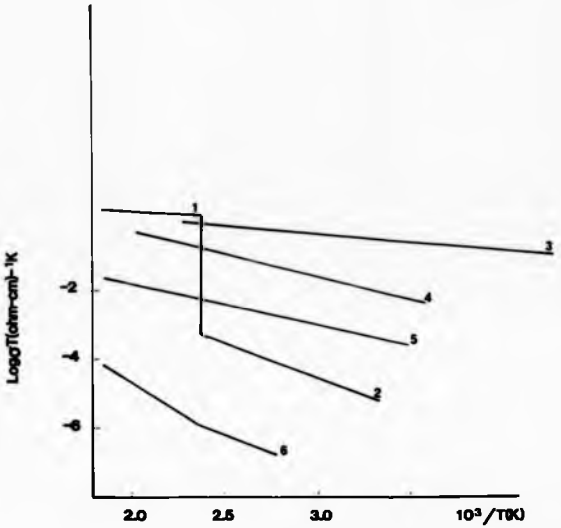

Fig. 1.1 Ionic conductivity of some fast ion conductors. Materials are: (1) α–AgI (2) β–AgI (3) $RbAg_4I_5$ (4) Na β–alumina (5) $L_{14}B_7O_{12}Cl$ (6) CuI (Chandra 1981)

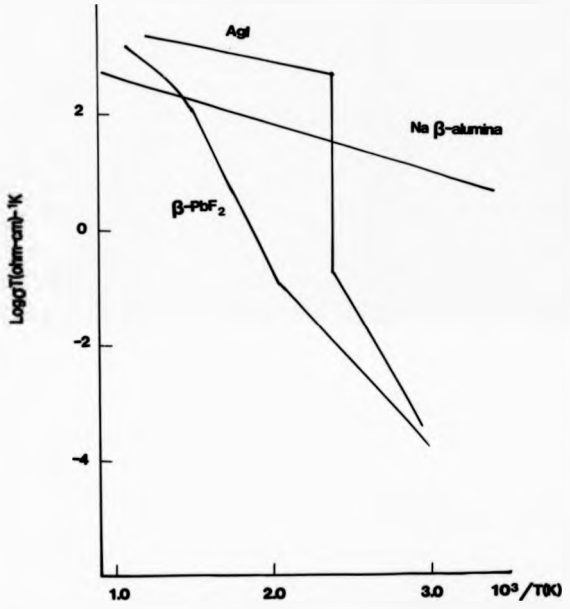

Fig. 1.2 Conductivity as a function of inverse temperature for the three types of fast ion conductors (Boyce et al 1977).

solids, e.g. alkali halides. Lidiard (1957) has shown that in a certain temperature range, the conductivity of ionic solids varies as

$$\sigma \sim 1/T \exp(-H_f/kT) \exp(-Ea/kT) \qquad (1.1)$$

where T is the absolute temperature, H_f is the energy of formation of a defect pair of either Frenkel or Schottky type, E_a is the activation enthalpy for migration of the mobile species and k is the Boltzmann constant. In some fast ion conductors the conductivity is not only high even at room temperature but varies very slowly with change of temperature, this means that the number of ions available for the conduction process is not only large but also fixed. As a consequence, the concept of thermally generated defects in such solids vanishes, and in equation (1.1) we take $H_f = 0$, thus the conductivity can be written as,

$$\sigma \sim 1/T \exp -Ea/kT \qquad (1.2)$$

A microscopic approach to explain the conduction mechanism in fast ion conductors was proposed by Rice and Roth (1972). The theory assumes an energy gap of ϵ_o in FIC, above which a localized ion is excited to a free-ion like state which propagates throughout the solid contributing to the different transport parameters. With this assumption Rice et al (1972) succeeded in obtaining expressions for the conductivity and thermo-electric power as

$$\sigma = 2/3\ [(Ze)^2/kTM]\ n_1\ \epsilon_o\ \tau_o \exp - \epsilon_o/kT \qquad (1.3)$$

and

$$Q = (k/Ze)\ \epsilon_o/kT \qquad (1.4)$$

where

Ze is the charge of the mobile ion

M is the mass of the mobile ion

n_1 is the number of available conducting ions per unit volume

τ_o is the lifetime of the ion in the free ion like state

Equation (1.3) has an Arrhenius type expression similar to the form of the conductivity obtained for the conventional ionic solids through hopping processes. Equation (1.4) predicts that the thermoelectric power is inversely proportional to T where the coefficient of proportionality is governed by ϵ_o, hence equation (1.4) can be written as

$$Ze\ TQ = \epsilon_o,$$

since the activation energy can be obtained from the conductivity measurement, a test to this model is to compare the activation energies obtained from the two measurements. The work of Takhashi et al (1970) and Shahi et al (1975) on few silver ion conductors have shown a good agreement for the activation energies obtained through the two techniques.

1.3 Alkali Metal Ion Conductors

The first alkali metal ion conductor, Na β-alumina was discovered by Yao and Kummer (1967). After that, research was very active in revealing more alkali ion conductors, especially the group studied by Huggins (Huggins 1977) at Stanford. The following review will concentrate on lithium ion conductors, fig.(1.3), because they are very promising materials for high energy density batteries due to the small ionic radius of Li^+ ion. According to Pauling the ionic radius of Li^+ is 0.60Å while that of Na^+ is 0.95Å. The handling of Li^+ is relatively easier and the work in this thesis also concerns the NMR of lithium ion conductors. A review of some lithium ion conductors will be explored from the conductivity viewpoint.

Compounds crystallizing with the fluorite structure such as β-PbF_2 and stabilized ZrO_2 show high ionic conductivity at elevated temperature. Raistrick et al (1976) tried to develop some lithium ion conductors with anti-fluorite structure to see if they exhibit analogous high ionic conductivity. One of these compounds is Li_5AlO_4 which was also

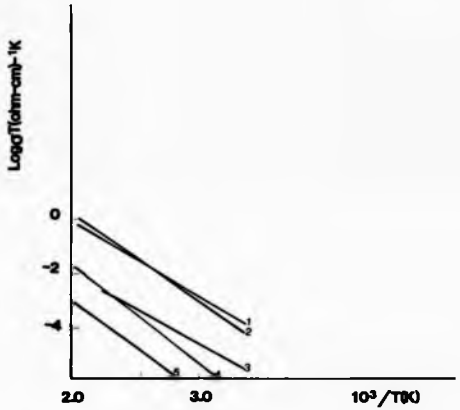

Fig.1.3 Ionic conductivity of some lithium ion conductors. Materials are: (1) Li_4SiO_4 (2) LiI (3) Li_2S (4) $LiAlSiO_4$ (5) Li_3N (Chandra 1981).

investigated by other techniques such as NMR. Differential thermal analysis (DTA) indicated that β↔α transition occurs at temperature of 340°C. The ionic conductivity measurements yielded a value of 2.3×10^{-7} $(\Omega\ cm)^{-1}$ at a temperature of 200°C, and showed an arrhenius temperature dependence giving an activation energy of 1.2eV. At temperature of 380°C conductivity started to increase rapidly over a range of 60 - 80°C obtaining the highest value of 0.3 $(\Omega\ cm)^{-1}$ at 450°C. Above 450°C, Li_5AlO_4 has a conductivity higher than the lithium or sodium β-alumina which qualifies it to be used in some high temperature battery systems.

Lithium Nitride, Li_3N is shown to be a relatively good fast ion conductor having room temperature conductivity of 3.7×10^{-8} $(\Omega\ cm)^{-1}$ (Huggins 1977, Bonkamp et al 1976). It belongs to class III in which conductivity exponentially grows from nonconducting to a conducting state without showing a phase transformation. Its crystal structure consists of Li_2N layers connected by lithium ions which form an N-Li-N bridge. This open structure provides large intersecting empty tunnels in two dimensions as a result of which Li^+ conduction is facilitated. The conductivity measurement was performed using the complex plane method in a frequency range between 20Hz to 50kHz and at various temperatures up to 500°C. The plot of conductivity versus the inverse of temperature yielded an activation energy of 0.61eV. The relatively high values of lithium ion conductivity in this material lead to the possibility of a practical use in the field of solid electrolytes in various lithium based systems.

The group of solids, boracites $Li_4B_2O_{12}$ X (X = Cl, Br, S), discovered by Reau et al (1978) are the best material for Li conduction apart from β-alumina. They are highly isotropic conducting lithium compounds which is an advantage over β-alumina which shows two dimensional conductivity due to its layer structure. One of these solids $Li_4B_2O_{12}$ Cl

has a conductivity of 10^{-2} $(\Omega\ cm)^{-1}$ at 300°C and its conductivity at 400°C is higher than that of β-alumina. The four Li ions occupy two sites, three occupy positions which are octahedrally co-ordinated and the fourth occupies a site which is tetrahedrally co-ordinated. The occupancy of the last site is 25% thus representing a structure which would allow large Li^+ ions transport.

$Li_4B_2O_{12}$ CL was also investigated through using CW and pulsed NMR by Reau et al (1979). The CW spectra revealed two peaks, one broad corresponding to the immobile Li^+ ions and a narrow one due to the diffusion of Li^+ ions. The pulsed NMR was performed at different frequencies measuring the spin lattice relaxation time in a temperature range up to 450°C. The low temperature part of T_1 yielded an activation energy of .28 eV, smaller than that obtained from the conductivity measurements, which is relatively common in fast ion conductors as shown in Table (1.2). At low temperatures, T_1 at different frequencies disagrees with the BPP model (see Chapter two) which assumes $T_1 \propto \omega_o^2$.

Lithium sulphate Li_2SO_4 exhibits high ionic conductivity at high temperature. It undergoes a phase transformation from β→α at a temperature of 573°C. This phase transition transforms Li_2SO_4 crystallographically from monoclinic at low temperature to FCC at high temperature (Kvist and Lunden (1965)). The high temperature FCC has a lattice parameter of 7.07Å at a temperature of 610°C Oye (1963) suggesting that for every sulphate ion there exists three cation sites, two tetrahedral sites with free space of 1.42Å and one octahedral site with a free space of 2.76Å. These free spaces allow Li^+ ions, which have a small radius to move through contributing to the conductivity.

Lithium orthosilicate Li_4SiO_4 is another lithium ion conductor at elevated temperature. It undergoes a phase transformation from insulating

to conducting rather slowly (West 1973), in the temperature range 600-725°C, attributed to the transformation occurring in several stages. The low phase conductivity is 2.4 x 10^{-10} $(\Omega\ cm)^{-1}$ at temperature of 25°C, while the high phase has a conductivity of 2.2 x 10^{-3} $(\Omega\ cm)^{-1}$ at 400°C. The activation energy obtained from the conducting phase is 0.74eV. Li_4SiO_4 has a monoclinic unit cell in which silicon is tetrahedrally coordinated to oxygen. There are 8 lithium ions per unit cell which are distributed among 18 lattice sites. An excess of sites over the number of conducting ions is a characteristic of FIC. It has been found that the substitution of SiO_4 by PO_4 or GeO_4 results in obtaining solids with higher ionic conductivity. Hu et al (1976) doped Li_4SiO_4 with Li_3PO_4 and investigated the conductivity as the mole % of Li_3PO_4 is changed. The results showed that with no Li_3PO_4 the Li_4SiO_4 has a conductivity of 1.3 x 10^{-9} $(\Omega\ cm)^{-1}$ at 100°C, while the compound containing 40 mole % of Li_3PO_4 has conductivity of 1.0 x 10^{-4} $(\Omega\ cm)^{-1}$ at the same temperature, which is five orders of magnitude higher.

1.4 NMR Studies of Fast Ion Conductors

NMR has proved to be a powerful tool in studying fast ion conductors particularly some ions of interest in the field of FIC such as Na^+, Li^+, F^-, etc. which can be investigated by NMR with relative ease due to their large nuclear magnetic moments. Shannon et al (1972) used NMR as a screening tool in which the linewidth is measured as a function of temperature. The narrowing of the linewidth is an indication of motion and hence the possibility of high conductivity in these materials. A number of recent review articles discussing the different aspects of NMR techniques in fast ion conductors are Bjorkstam et al (1980), Richards (1979), Whittingham et al (1977) and Boyce et al (1977).

If an atom moves, the internal fields change which results in the

nuclei experiencing a fluctuating field of magnetic or electrical origin. These fluctuating fields cause spin flip transitions affecting the spin lattice relaxation time T_1 and also the motion averages the interactions responsible for spin-spin relaxation time T_2. Assuming that the correlation function of the fluctuating field is an exponentially decaying function with a characteristic time τ_c, the BPP model (Bloembergen, Purcell and Pound 1948) predicts that for nuclear dipolar interactions T_1 and T_2 are given by

$$\frac{1}{T_1} = C\left[\frac{\tau_c}{1+\omega_0^2\tau_c^2} + \frac{4\tau_c}{1+4\omega_0^2\tau_c^2}\right]$$

$$\frac{1}{T_2} = C\left[\frac{3}{2}\tau_c + \frac{5}{2}\frac{\tau_c}{1+\omega_0^2\tau_c^2} + \frac{\tau_c}{1+4\omega_0^2\tau_c^2}\right], \qquad (1.5)$$

where C is a constant defining the interaction strength and ω_0 is the Larmor frequency. Fig. (1.4) shows the variation of T_1 and T_2 as a function of correlation time. At the minimum of T_1 we have $\omega_0 \cdot \tau_c^{-1}$ and at high temperature we have

$$1/T_1 = 1/T_2 \propto \tau_0 \exp Ea/kT,$$

assuming that the motion is thermally activated. Therefore the slope of the logarithm of $1/T_{1,2}$ versus 1/T curve should yield the activation energy Ea, with the hopping rate obtained from the T_1 minimum. These are the two most important constants. The knowledge of the hopping rate helps to give an estimate of the ionic conductivity through the Nernst-Einstein relation which has the form

$$\sigma(0) = N(Ze)^2 D/kT \qquad (1.6)$$

where N is the number of ions/volume, Ze is the valence of the conducting charge and D is the coefficient of diffusion which can be expressed as

$$D = \nu\ell^2/2d,$$

where ℓ is the jump length, d is the dimension of the system and ν is the hopping rate obtained from NMR measurements.

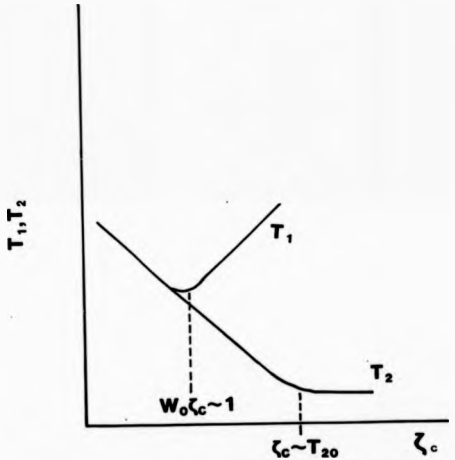

Fig.1.4 Typical variation of NMR relaxation times as a function of correlation time.

The materials investigated in this thesis belong to group iii of fast ion conductors. A few representative solids will be reviewed. The NMR data obtained from different researchers seem to indicate some characteristic points.

(i) T_1 exhibits a minimum in T_1 versus 1/T curve. But in the low temperature part of T_1, the frequency dependence of T_1 does not follow BPP model which states $T_1 \alpha \omega_o^2$ whereas the observations show that $T_1 \alpha \omega_o^{\alpha}$, where α is a constant less than 2.

(ii) The attempt frequency which is defined as the vibrational frequency of the mobile ion residing in a potential well between hops was found to be much lower than the phonon frequency. Also the activation energy obtained through NMR was smaller than that obtained from the conductivity, tables (1.1 and 1.2).

(iii) Traces of paramagnetic impurities have a marked effect on the relaxation processes.

1.5 Lithium NMR Studies

Follstaedt et al (1978) studied β-Li_5AlO_4 by measuring T_1 at three different frequencies of 7.2, 12.7 and 21.5MHz and T_2 at 21.5MHz, in a temperature range from 20°C to 500°C. The low temperature part of T_1 yielded an activation energy of 0.56eV while T_2 gives 0.63eV from the motional narrowing region. At the minimum of T_1 where $\omega_o\tau_c \sim 1$, a value of 2×10^{12} sec^{-1} is obtained for the attempt frequency which is close to the optical phonon frequency. T_1 shows a strong frequency dependence as $T_1 \alpha \omega_o^{1.8}$ instead of the BPP model which gives $T_{1_o} \alpha \omega^2$. To identify the mechanism responsible for the relaxation process, at the T_1^{-1} maximum was calculated on the basis that the interaction is dipolar between the diffusing lithium ions. The value found for at the T_1^{-1} max accordingly

was about 5 sec^{-1} at 21.5MHz while experimentally it was 5 x 10^2 sec^{-1}, which requires a stronger interaction. Since ^7Li has a spin of $^3/_2$, relaxation due to quadrupolar interactions is a possibility, but this requires that the ratio T_1/T_2 = 1 at high temperature which unfortunately was not fulfilled. Experimentally T_1/T_2 - 4, an indication that the relaxation is due to paramagnetic ions. An EPR experiment was performed on the sample which gave the strongest signal at g = 2. That signal was attributed to Fe^{3+} in the Al^{3+} positions. Comparing the intensity of the signal with that of standard sample an estimate of 150ppm of Fe^{3+} was assumed to be contained in the compound of β-Li_5AlO_4. With this information the data was fitted to a model based on a dipolar interaction between the nuclear moment of lithium and the moment of Fe^{3+}. This model yields T_1^{-1} max as 6 x $10^2 sec^{-1}$ compared with the experimental value of 5 x 10^2 sec^{-1}. Also T_2^{-1} at the start of the motional narrowing is 4 x 10^3 sec^{-1} while the experimental value is 10^4 sec^{-1}. A complete treatment of T_1 and T_2 over the whole temperature range was performed by Richards' (1978) discussed in Chapter two of this thesis.

Follstaedt et al (1976) measured T_1 for ^7Li in β-$LiAlSiO_4$ at a frequency of 8MHz and also used T_1 data of the same material prepared and measured by Weaver et al (1976) at a frequency of 20MHz. The measurements showed that T_1 is independent of frequency at temperatures below T_1min. The interpreta- tion put forward is the existence of motion between two wells with depth Δ_A and Δ_B. This correlated one dimensional motion is supported by the conductivity data which gives an anisotropy of 10^3. The previous notion is considered to be responsible for the relaxation mechanism and the spin lattice relaxation rate is

$$T_1^{-1} \propto \exp[-(\Delta_A - 2\Delta_B)/kT] \qquad (1.7)$$

Equation. (1.7) predicts that T_1 is frequency independent as shown

experimentally. The minimum in T_1 for β-$LiAlSiO_4$ has nothing to do with $\omega_o\tau_c \sim 1$ since there is no frequency dependence, hence it was assumed that an order-disorder phase transition occurred at this temperature. Unfortunately, no phase transition has been observed in this material through DTA.

Dupree et al (1983) measured T_1 and T_2 for ^7Li in LiI and LiI/Al_2O_3 at two Larmor frequencies of 12.3 and 7.5MHz in the temperature range up to 430°C. T_1 showed a variation with the change of temperature giving a minimum at 330°C. Below the minimum the T_1 curve yielded an activation energy of 0.58eV not far from 0.43eV obtained by conductivity measurements (Schlaikyer et al (1973). The hopping rate obtained from the T_1 minimum was used in the Nernst-Einstein relation to estimate a value for the conductivity at that temperature of 3.3×10^{-4} $(\Omega\ cm)^{-1}$, which compares favourably with the conductivity measurements. LiI/Al_2O_3 showed the same trend as LiI with change of temperature having the same minimum at 330°C. The values of T_1 were shorter than those of LiI, possibly due to the existence of some impurities. The relaxation mechanism in the pure LiI was considered to be dipolar in origin. Although Li^+ ion has a quadrupole moment, quadrupolar interaction was excluded as a source of relaxation. Paramagnetic impurities were thought to be ineffective on the grounds that in order to effect relaxation processes, the concentration of the impurities should be in the range of a few hundreds of ppm.

The solid solution between Li_4SiO_4 and Li_3PO_4 as indicated previously was found by Hu et al (1976) to be one of the best lithium ion conductors. Takeshi et al (1980) studied $Li_{4-x}(PO_4)_x(SiO_4)_{1-4}$ where $0 \leq x \leq .35$. Three samples of x = .1, .2 and .35 were investigated using NMR. The spin lattice relaxation time of ^7Li was measured in the temperature range between -70°C and 440°C at a frequency of 23.315MHz. T_1 versus 1/T

curve for x = .35 shows the usual trend where T_1 decreases with increase of temperature showing a minimum at 230°C. Below the minimum two components of the slope were observed; this is obvious from the differential thermal analysis which showed the existence of two phases at 45°C and 180°C. With the use of activation energy at T < 180°C which is 1.4eV, an estimate of the attempt frequency of 0.9 x 10^{12} sec^{-1} was obtained. The activation energy found was smaller than that obtained from the conductivity which could be related to some short range motion affecting the NMR relaxation. The other samples with x = .1 and .2 showed the same trend as in the case of x = .35 only shifted the curve toward the high temperature part. The activation energy showed a decrease with increasing x, since for more Li_3PO_4 dissolved in Li_4SiO_4 lattice, more vacancies are introduced in the Li^+ ion sites. To explain the mechanisms of the relaxation processes, Takeshi assumed that in the high temperature part of T_1, the relaxation is through the fluctuating electric field gradient caused by diffusion of Li^+ ions. We feel another possibility for relaxation is the role of paramagnetic ions, but unfortunately they were not able to carry out T_2 measurements where the ratio T_1/T_2 helps in determining the type of relaxation.

1.6 Lithium Fast Ion Conductors Studied in this Thesis

a) Dilithium Trititanate $Li_2Ti_3O_7$

This compound aroused some controversy due to its frequency independent T_1 and the low value of the prefactor as of 4 x 10^7 sec^{-1}, which led Huberman and Boyce (1978) to formulate their theory about the breakdown of the absolute rate theory. Also the work of Richards (1978) which is based on considering $Li_2Ti_3O_7$ as a one-dimensional conductor was rejected by Boyce et al (1979) on the basis of low anisotropy obtained through the conductivity data. These anomalies had been shown by a few

fast ion conductors, and $Li_2Ti_3O_7$ is a good candidate for reinvestigation of these effects in the hope of putting forward some explanation without the need for the breakdown of the absolute rate theory or the need to consider $Li_2Ti_3O_7$ as a one dimensional ionic conductor.

b) Li_2TiO_3

This compound represents one of the LiTiO group. Although no detailed study of the conductivity has been performed on it, the structural study by Huggins et al (1973) excluded the possibility of it being a fast ion conductor. It was hoped to observe motional narrowing in some temperature range which could indicate some conduction. The NMR data would give some dynamical parameters which would help other experimental techniques to reveal its conduction mechanism.

c) The Lisicon Group

The high ionic conductivity of this group of materials at a temperature of 300°C, encouraged a few researchers to use different techniques to study their properties. Only one NMR investigation by Bose et al (1986) was carried out. This study did not elaborate on the different aspects of NMR parameters. The lack of NMR data on these materials is remedied by the study carried out in this thesis on $Li_{12}Mg_2(SiO_4)_4$ and $Li_{12}Zn_2(SiO_4)_4$.

Table (1.1) Attempt frequency ν_o measured by NMR for some lithium ion conductors

Compound	$\nu_o(sec)^{-1}$	Method	Reference
$LiAlSiO_4$	5×10^7	line narrowing	Follstaedt (1976)
$\gamma Li_{1.12}V_3O_{3.9}$	4×10^{10}	"	Halstead (1973)
$Li_{2.15}B_{0.15}C_{0.85}O_3$	10^8	"	Shannon (1977)
$Li_2Ti_3O_7$	4×10^7	"	Haberman (1978)
$Li_2Ti_3O_7$	10^{10}	T_1 min.	This thesis
Li_5AlO_4	2×10^{12}	"	Follstaedt (1978)
$Li_{12}Mg_2(SiO_4)_4$	1×10^{12}	"	This thesis
$Li_{12}Zn_2(SiO_4)_4$	4.7×10^{11}	"	"
$Li_{12}Zn_2(GeO_4)_4$	1.18×10^{12}	"	Bose (1986)
$Li_{14}Zn(GeO_4)$	2.13×10^{12}	"	"

Table (1.2) Activation energies determined by NMR and conductivity measurements in the same temperature range.

Compound	E_{NMR} ev	Reference	E_{Cond} ev	Reference
$LiALSiO_4$	0.8	Follstaedt (1976)	0.7	Alpen (1979)
$Li_{4.2}Si_{0.8}Al_{0.2}O_4$	0.2	Shannon (1977)	0.4	Shannon (1977)
$Li_2Ti_3O_7$	0.2	Huberman (1978)	0.44	Boyce (1978)
$Li_2Ti_3O_7$	0.4	This thesis	0.44	"
LiI	0.58	Dupree (1983)	0.44	Schlaikyer (1973)
$Li_{12}Zn_2(GeO_4)_4$	0.37	Bose (1986)	0.24	Majumdar (1983)
$Li_{14}Zn(GeO_4)_4$	0.43	"	0.25	Hong (1978)
$Li_{12}Mg_2(SiO_4)_4$	0.50	This thesis		
$Li_{12}Zn_2(SiO_4)_4$	0.43	"		

CHAPTER TWO

NMR THEORETICAL FRAMEWORK

Introduction

Nuclear magnetic resonance (NMR) is a powerful tool for investigation of fast ion conductors as this technique allows one to look into the material by using the conducting ion as a probe. The basic interactions encountered in the study of the properties of fast ion conductors will be reviewed. The nucleus of interest must have a spin greater than zero and the spin system is described by a Hamiltonian of the form:

$$H = H_z + H_D + H_Q + H_p \qquad (2.1)$$

where H_z is the Zeeman interaction of the nucleus with the applied magnetic field

H_D is the dipolar interaction

H_Q is the quadrupolar interaction for nuclei with a spin > $\frac{1}{2}$

H_p is the interaction between an unpaired electron and the nucleus which could be the result of the existence of paramagnetic ions in the material.

2.1 The Zeeman Interaction

This represents the interaction between the spins and the external magnetic field directed along the z axis. If the nucleus has a magnetic moment μ, then the interaction can be expressed

$$H_z = -\bar{\mu} \cdot \bar{B}_o = \gamma \hbar B_o I_z \qquad (2.2)$$

where γ is known as gyromagnetic ratio and I_z is the operator corresponding to the z-component of the total spin state. The eigenvalues of the

Zeeman Hamiltonian are

$$E_m = -\gamma\hbar\, m\, B_o, \tag{2.3}$$

m takes (2I + 1) values from I to -I. Transition between adjacent energy levels can be stimulated by radiation with an angular frequency ω such that,

$$E = \hbar\omega \tag{2.4}$$

or

$$\omega = \gamma B_o \tag{2.5}$$

known as the resonance equation.

Relaxation

Relaxation is a process in which the spin system transforms from a nonequlibrium to an equilibrium state. The rate for the spin system to reach equilibrium is governed by T_1 and T_2 known as the spin lattice and spin-spin relaxation times.

A process that leads to relaxation is the existence of a fluctuating local field which could exist from various sources. A magnetic field produced by one nucleus at the site of another nucleus via dipolar coupling will be one source of relaxation. Another process playing an important role is the quadrupolar interaction which occurs for spin $I > \frac{1}{2}$, that represents the interaction of the electric field gradient with the quadrupole moment, this fluctuating electric field causes transitions between energy levels once it has a component of the required frequency. Another important source of relaxing a nucleus is by paramagnetic ions where the unpaired electron creates a fluctuating magnetic field which relaxes the ion and provides a comparatively short relaxation time.

The fluctuating field of whatever source is denoted by f and its ability to relax the spins depends on the fluctuation having frequencies close to the Larmor frequency of the resonating spins. We introduce the

autocorrelation function G(τ) which can be defined by (Abragam (1961)).

$$G(\tau) = \overline{f(t)\, f(t+\tau)} \tag{2.6}$$

G(τ) is not a function of t but correlating the motion at a certain instant with that at a later time. G(τ) is a time domain function and to switch to the frequency domain, we must use the spectral density function J(ω) where,

$$J(\omega) = \int_{-\infty}^{\infty} G(\tau)\, e^{-i\omega\tau}\, d\tau, \tag{2.7}$$

The spectral density function defines the strength of the fluctuation at a certain frequency. Thus

$$G(\tau) = \frac{1}{2\pi} \int_{-\infty}^{\infty} J(\omega)\, e^{i\omega\tau}\, d\omega \tag{2.8}$$

At τ = o we have

$$G(o) = |\overline{f(o)}|^2 = \frac{1}{2\pi} \int_{-\infty}^{\infty} J(\omega) d\omega \tag{2.9}$$

where $\overline{f(o)}^2$ is porportional to the energy corresponding to the component f(t). Relaxation times give us information about the strength and the time dependence of the field fluctuation, the two kinds of relaxation tell us about two aspects of the spin system. The spin lattice relaxation time involves a flow of energy from the spin system to the lattice, while the spin spin relaxation time concerned with the redistribution of energy within the system of resonating spins.

2.2 Dipole-Dipole Interaction

The energy of interaction between two dipoles of moments $\bar{\mu}_1$ and $\bar{\mu}_2$, separated by a distance r is U given by

$$U = \frac{\mu_o}{4\pi} \left(\frac{\bar{\mu}_1 \cdot \bar{\mu}_2}{r^3} - \frac{3(\bar{\mu}_1 \cdot \bar{r})(\bar{\mu}_2 \cdot \bar{r})}{r^5} \right) \tag{2.10}$$

Treating the dipole moment as a quantum mechanical operator such as

$$\bar{\mu}_1 = \gamma_1 \hbar \bar{I}_1 \quad \text{and} \quad \bar{\mu}_2 = \gamma_2 \hbar \bar{I}_2$$

The contribution to the Hamiltonian becomes

$$H_D = \left(\frac{\mu_o}{4\pi}\right) \gamma_1 \gamma_2 \hbar^2 \left(\frac{\bar{I}_1 \cdot \bar{I}_2}{r^3} - \frac{3(\bar{I}_1 \cdot \bar{r})(\bar{I}_2 \cdot \bar{r})}{r^5} \right)$$

If we consider a large number of interacting spins then,

$$H_D = \left(\frac{\mu_o}{4\pi}\right) \sum_{j \neq k} \frac{\gamma_j \gamma_k \hbar^2}{r_{jk}^3} \left(\bar{I}_j \cdot \bar{I}_k - \frac{3(\bar{I}_j \cdot \bar{r})(\bar{I}_k \cdot \bar{r})}{r^2} \right) \qquad (2.11)$$

which is written in terms of spherical polar coordinates as,

$$H_D = \left(\frac{\mu_o}{4\pi}\right) \sum_{j \neq k} \frac{\gamma_j \gamma_k \hbar^2}{r_{jk}^3} (A + B + C + D + E + F) \qquad (2.12)$$

where

$$\begin{aligned}
A &= \bar{I}_{jz}\bar{I}_{kz} \ (3\cos^2\theta - 1) \\
B &= \tfrac{1}{4}(1 - 3\cos^2\theta)(\bar{I}_{j+}\bar{I}_{k-} + \bar{I}_{j-}\bar{I}_{k+}) \\
C &= -\tfrac{3}{2} \sin\theta \cos\theta \exp(-i\phi)(\bar{I}_{jz}\bar{I}_{k+} + \bar{I}_{j+}\bar{I}_{kz}) \\
D &= -\tfrac{3}{2} \sin\theta \cos\theta \exp(-i\phi)(\bar{I}_{jz}\bar{I}_{k-} + \bar{I}_{j-}\bar{I}_{kz}) \\
E &= -\tfrac{1}{4} \sin^2\theta \exp(-2i\phi)\ \bar{I}_{j+}\bar{I}_{k+} \\
F &= -\tfrac{1}{4} \sin^2\theta \exp(2i\phi)\ \bar{I}_{j-}\bar{I}_{k-},
\end{aligned} \qquad (2.13)$$

where θ and ϕ are the polar and azimuthal angles, r_{jk} is the distance between the spin j and k and $\bar{I}_+$, $\bar{I}_-$ are the raising and lowering operators. The term A is proportional to the term $\bar{I}_{jz}\bar{I}_{kz}$, it connects $|m_1,m_2>$ with $<m_1,m_2|$, term B is proportional to the term $\bar{I}_{j+}\bar{I}_{k-} + \bar{I}_{j-}\bar{I}_{k+}$ which connects $|m_1,m_2>$ to the states $<m_1+1,\ m_2-1|$ or $<m_1-1,\ m_2+1|$, the sum of the two eigenvalues m remains unchanged. The effect of this term is to flip one spin in one direction while the other spin is flipped in the opposite direction, the process is known as flip flop. The effect of terms C and D is to flip one spin only, they connect $|m_1,m_2>$ to $|m_1+1,m_2>$ or $|m_1,m_2+1>$. The last terms E and F flip both spins in the same direction i.e. the state $|m_1,m_2>$ into $|m_1+1,m_2+1>$ or $|m_1-1,m_2-1>$. The terms C to F have a weak effect on the Hamiltonian so are usually neglected and the Hamiltonian containing only terms A and B is called a truncated

Hamiltonian.

After considering the dipole dipole interaction, we examine the rates T_1^{-1} and T_2^{-1} in this formalism which is given by Abragam (1961).

$$T_1^{-1} = \frac{3}{2}\gamma^4\hbar^2\, I(I+1)[J_1(\omega_0) + J_2(2\omega_0)] \tag{2.14}$$

$$T_2^{-1} = \frac{3}{8}\gamma^4\hbar^2\, I(I+1)[J_0(0) + 10J_1(\omega_0) + J_2(2\omega_0)] \tag{2.15}$$

In the case of the dipole dipole interaction the fluctuating field has the components f_0, f_1, f_2 as

$$f_0 = \frac{1-3\cos^2\theta}{r^3}, \tag{2.16}$$

$$f_1 = \frac{\sin\theta\cos\theta e^{-i\phi}}{r^3}$$

$$f_2 = \frac{\sin\theta e^{-i\phi}}{r^3}$$

Using the BPP approximation which assumes a correlation function decaying as exp $-|\tau|/\tau_c$, in which τ_c is the correlation of motion, this yields

$$J(\omega) = \overline{f^2}\,\frac{\tau_c}{1+\omega^2\tau_c^2} \tag{2.17}$$

With this form of the spectral density function, the rates T_1^{-1} and T_2^{-1} take the form

$$T_1^{-1} = \Omega\left[\frac{\tau_c}{1+\omega_0^2\tau_c^2} + \frac{4\tau_c}{1+4\omega_0^2\tau_c^2}\right] \tag{2.18}$$

$$T_2^{-1} = \Omega\left[\frac{3}{2}\tau_c + \frac{5}{2}\,\frac{\tau_c}{1+\omega_0^2\tau_c^2} + \frac{\tau_c}{1+4\omega_0^2\tau_c^2}\right] \tag{2.19}$$

where Ω is the Van Vleck second moment. It is worth investigating the BPP expressions at low and high temperatures.

(i) At high temperature where $\omega_0\tau_c \ll 1$, equations (2.18) and (2.19) yield

$$T_1^{-1} = T_2^{-1} = 5\,\Omega\,\tau_c$$

This region where both rates are equal is known as the motional narrowing region. The relaxation rates are proportional to τ_c and if we take the logarithm of the rates we get

$$\ln T_1 = \ln T_2 = -\ln (5\Omega\tau_o) - Ea/kT$$

$\ln T_1$ or $\ln T_2$ versus $1/T$ gives a straight line with a slope giving the activation energy Ea.

(ii) At low temperature where $\omega_o\tau_c >> 1$, equation (2.18) yields.

$$T_1^{-1} = \frac{2\Omega}{\omega_o^2\tau_c} \qquad (2.20)$$

Equation (2.20) shows that in this temperature range the rate of T_1 is proportional to ω_o^2 and taking the logarithm of both sides of equation (2.18) we get

$$\ln T_1 = \ln \frac{\omega_o^2\tau_o}{2\Omega} + \frac{Ea}{kT},$$

hence the activation energy is obtained from the slope of $\ln T_1$ versus $\frac{1}{T}$ curve.

(iii) An important feature from $\ln T_1$ versus $1/T$ curve is that there is a minimum at $\omega_o\tau_c = 1$. Assuming the previous processes to be thermally activated with an Arrhenius relationship,

$$\tau_c = \tau_o e^{Ea/kT} = 1/\omega_o,$$

and τ_o can be calculated. This is the inverse of the attempt frequency which can be compared with the value obtained using other experimental techniques.

The Second Moment

The exact line shape of an nmr spectra is not in general calculable theoretically, but a method developed by Van Vleck (1948) using an expansion technique in terms of moments of the line yields some structural information. Assuming a line shape function $f(\omega)$, the second moment is given by

$$\Omega = \int_{-\infty}^{\infty} (\omega-\omega_o)^2 f(\omega)\, d\omega \qquad (2.21)$$

In the case of the line shape $f(\omega)$ having a Gaussian shape, then

$$\Omega = T_2^{-2},$$

while for a Lorentzian line shape, the integral of equation (2.21) diverges, but truncation of the integral to the range $-\alpha<\omega<\alpha$, yields a reduced second moment given by

$$\Omega = \frac{2\alpha}{\pi T_2^2}$$

If we have N identical nuclei with spin I at distances r_{jk} for a polycrystalline sample, the second moment is given by Abragam (1961)

$$\Omega = \frac{3}{5}\gamma^4\hbar^2 I(I+1)\sum_{j\geq k} r_{jk}^{-6}/N \qquad (2.22)$$

One use of the second moment is that if the interaction is dipolar, then it is a measure of the internuclear distances in the sample. When $1/\tau_c$ is small then the NMR linewidth is equal to $\Omega^{\frac{1}{2}}$. As $1/\tau_c$ increases and becomes comparable with the linewidth we get the region of motional narrowing, at the start of which $\Omega^{\frac{1}{2}} \sim 1/\tau_c$.

2.3 Quadrupolar Interaction

For nuclei with spin $I > \frac{1}{2}$ including lithium and sodium, the nuclear charge distribution deviates from spherical symmetry resulting in a quadrupole moment eQ defined as

$$eQ = \int \rho(r)(3z^2-r^2)d^3r$$

The integration is carried out over the charge density $\rho(r)$, and z is the direction defined by the nuclear spin.

The motion of an ion in the lattice creates a fluctuating electric field gradient at the position of the relaxing nucleus which may constitute an important mechanism for relaxation. Assuming the interaction is a perturbation on the Zeeman energy and the correlation function is an exponentially decaying function with time, then the relaxation rates expressed in terms of the spectral density functions according to Abragam (1961) are

$$T_{1Q}^{-1} = \frac{3}{20}\frac{2I+3}{I^2(2I-1)}\left(\frac{e^2Qq}{\hbar^2}\right)^2(1+\eta^2/3)[J_1(\omega_0)+4J_2(2\omega_0)] \qquad (2.23)$$

$$T_{2Q}^{-1} = \frac{3}{40}\frac{2I+3}{I^2(2I-1)}\left(\frac{e^2Qq}{\hbar^2}\right)^2 (1+\eta^2/3)[3J_0(o) + 5J_1(\omega_0) + 2J_2(2\omega_0)] \quad (2.24)$$

where eq is defined as the field gradient V_{zz} and η is called the asymmetry parameter, which measures the deviation of the electric field gradient from axial symmetry and is defined as:

$$\eta = \frac{V_{xx} - V_{yy}}{V_{zz}} \qquad 0 \leq \eta \leq 1$$

In the high temperature limit where $\omega_0\tau_c < 1$, then equations (2.23) and (2.24) reduce to

$$T_1^{-1} = T_2^{-1} = \frac{3}{40}\frac{2I+3}{I^2(2I-1)}\left\{\frac{e\,Q\,q}{h}\right\}^2 (1+\eta^2/3)\,\tau_c, \quad (2.24')$$

equation (2.24') shows the trends in the dependence of the relaxation rates on experimental parameters such as the temperature and the coupling constant.

2.4 Interaction with Paramagnetic Ions

The interaction of an electron with the nucleus is represented by a Hamiltonian H given by

$$H = -\gamma_I\gamma_e\hbar^2\left[\left(\frac{\bar{I}\cdot\bar{S}}{r^3} + \frac{3(\bar{I}\cdot\bar{r})(\bar{s}\cdot\bar{r})}{r^5}\right)_{dip} + \left(\frac{8\pi}{3}\,\bar{I}\cdot\bar{S}\,\delta(r)\right]_{contact}\right] \quad (2.25)$$

For conduction electrons in metals the contact part of the Hamiltonian plays the dominant role in the relaxation processes and the dipolar interaction is considered to be relatively weak. In ionic solids when contaminated with paramagnetic ions, the unpaired electron interacts with the nuclei either through dipole dipole or contact interactions. To consider the first part of equation (2.25) which represents the dipolar interaction, this term as shown previously in equation (2.13) contains one operator which flips the nuclear spin and leaves the electron spin unchanged. This process is favourable because it requires an energy of $\hbar\omega_I$ which is smaller than if both spins are changed which requires an

energy of $\hbar(\omega_S \pm \omega_I)$. This operator is appropriate to use in the case of ionic solids having some paramagnetic ions. The operator is given as

$$G = -\frac{3}{2}\sin\theta\cos\theta\, e^{i\phi}\, S_z I_+,$$

with this operator, the spin lattice relaxation rate is given by Abragam (1961) neglecting the angular dependance

$$T_1^{-1} \sim k/r^6 \tag{2.26}$$

where $$k = \frac{2}{5}\gamma_s^2\gamma_I^2\hbar^2 S(S+1)\frac{\tau}{1+\omega_o^2\tau^2} \tag{2.27}$$

and γ_S, γ_I are the gyromagnetic ratios of the electron and the nucleus respectively, s is the spin of the electron, ω_I is the Larmor frequency of the nucleus, r is the distance between the electron and the nuclear spin and τ is the longitudinal electron relaxation time.

Follstaedt et al (1978) in his investigation of $Li_5A\ell O_4$ used equation (2.26) to show that the relaxation time manifested in $Li_5A\ell O_4$ is due to dipolar interaction and modified equation (2.26) slightly to accommodate the paramagnetic impurity concentration c. The relaxation rate used by Follstaedt et al (1978) has the form

$$T_1^{-1} = \frac{2}{5}c\hbar^2\gamma_I^2\gamma_s^2 s(s+1)\frac{\tau_c}{1+\omega_o^2\tau_c^2}\sum_n \frac{1}{r_n^6}, \tag{2.28}$$

This equation assumes that the motion of the diffusing ion is rapid enough to make $\tau_c < \tau$ so that τ_c governs the relaxation.

The previous formalism is valid when the distance between the paramagnetic impurity and the nucleus is a few angstroms. In the case of a larger distance the interaction is by a different mechanism known as spin diffusion, which occurs through the mutual flips between neighbouring spins and is governed by the diffusion equation. This equation in the presence of paramagnetic impurities can be expressed as

$$\frac{\delta P}{\delta t} = D\Delta P - k\sum_n \frac{1}{|r-r_n|^6}(P-P_o) - 2AP, \tag{2.29}$$

where p is the nuclear polarization, A is the rate at which the spin flips, r_n are the positions of the impurities and D is the diffusion constant. Relating T_1 to 2A, then an expression for the spin lattice relaxation time is written

$$T_1 = \frac{1}{4\pi c\ b\ D} \quad , \tag{2.30}$$

where c is the impurity concentration, b is defined as

$$b = \left(\frac{k}{D}\right)^{\frac{1}{2}} \quad ,$$

in which k is given by equation (2.27) and represents the direct relaxation to that characterized by spin diffusion.

Richards (1978) developed a theory to account for the paramagnetic impurity interaction in fast ion conductors. It assumes nearest neighbour hyperfine interactions as the dominant source of relaxation and makes separate predictions for T_1 and T_2 in terms of ν, the ionic hopping rate, ω_e, ω_n the electronic and nuclear Larmor frequencies and τ_e the electronic relaxation time. This formalism is successful in accounting for some experimental data such as the existence of a single peak in T_2 and two peaks in T_1.

Assuming that the diffusing nucleus experiences a time dependent interaction.

$$H'(t) = \hbar \sum_{\alpha,\beta} A_{\alpha\beta}\ S_\alpha(t)\ I_\beta, \tag{2.31}$$

where $S_\alpha(t)$ and I_β are components of the electronic and nuclear spins, respectively. This interaction is used as a perturbation in a theory developed by Kubo-Tomita (1956). One requirement for the validity of the perturbation approximation is that $A\tau_c < 1$, where A is the interaction and τ_c is the duration of the nn encounter. If the inequality does not hold then the perturbation breaks down. This interaction could be the transferred hyperfine (contact) interaction as used in the case of $Mn:PbF_2$

or the dipolar interaction as demonstrated in interpreting data for Li_5AlO_4. The time dependence of equation (2.31) arises from the ion diffusion which transports ions to lattice sites where $H'(t) \neq 0$, and from the time dependence of $S_\alpha(t)$. The rate equations in this formalism can be expressed as:

$$T_\alpha^{-1} = (1 - < f_\alpha >) zc\nu, \tag{2.32}$$

where

α is 1 or 2 referring to T_1 and T_2, Z is the number of nearest neighbours to a paramagnetic ion, c is the concentration of paramagnetic ions and $<f_\alpha>$ is the average relaxation function which has the form

$$<f_\alpha> = \nu \int_0^\infty e^{-\nu\tau} f_\alpha(t)\, dt\ , \tag{2.33}$$

and

$$f_\alpha(t) = \exp\left\{ - \int_0^\tau (\tau - t) G_\alpha(t) dt \right\} \tag{2.34}$$

where $\nu e^{-\nu\tau} d\tau$ is the probability that the ion hopping at a rate ν will reside

at a site for a time between t and t + dτ and $G_\alpha(t)$ is the correlation function which depends on the interaction A and the parameters ω_e, ω_n and τ_c. Two examples using different interaction mechanisms are illustrated below.

(i) Transferred hyperfine interaction

This interaction of the form $\hat{A}\ A\ \vec{I}.\vec{S}$ is used to interpret the data for PbF_2 doped with Mn^{2+} Hogg et al (1977). The appropriate correlation functions are,

$$G_1(t) = \frac{2}{3} A^2 S(S+1) \cos \omega_e t\ e^{-t/\tau_c}$$

$$G_2(t) = \frac{1}{3} A^2 S(S+1)(1 + e^{-i\omega_e t}) e^{-t/\tau_c}$$

these correlation functions give rise to relaxation functions of the form

$$<f_1> = \int_0^\infty du\, e^{-u} \exp\left[y\left[\frac{1}{x^2} (\cos ux - 1) \right] \right]$$

$$\langle f_2 \rangle = \mathrm{Re} \int_0^\infty du\, e^{-u} \exp[-y\,(u - \frac{iu}{x} + \frac{1 - e^{-iux}}{x^2})] \qquad (3.35)$$

with $y = 1/3\ A^2\ s(s+1)/\tau_c$, $x = \omega_e/\nu_c$. To fit the T_2 data obtained by Hogg et al (1977), equation (3.35) is substituted into equation (3.32). To get the fit shown in fig. (2.1), the parameters are chosen as $A = 1.5 \times 10^8\ \mathrm{sec}^{-1}$, $C = 3 \times 10^{-4}$, $z = 4$, $\omega_e = 10$ GHz and $1/\nu_c$ is taken from the conductivity data of Boyce et al (1977). The solid line fits the data quite well giving the features of a maximum and a minimum in T_2^{-1}.

(ii)Dipolar Interaction

In Li_5AlO_4 Follstaedt et al (1978) observed that at high temperature the ratio $T_1/T_2 \sim 4$ indicating a relaxation by paramagnetic ions. Although the compound was formed from pure materials, EPR indicated the existence of Fe^{3+} with a concentration of 150ppm. These Fe^{3+} ions were assumed to be replacing some Al^{3+} in the material. They calculated T_1 min. using equation (2.28) and found good agreement. Richards' used this data to test his theory. The interaction was assumed to be electron-nucleus dipole coupling, and the correlation functions for T_1 and T_2 have the form

$$G_1(t) = \frac{2}{3} S(S+1)\, \gamma_I^2\, \gamma_S^2\, \hbar^2\, r^{-6} \cos \omega_o t\ e^{-t/\tau_c}$$

$$G_2(t) = \frac{1}{5} s(s+1)\, \gamma_I^2\, \gamma_S^2\, \hbar^2\, r^{-6}\, e^{-t/\tau_c} + 2\,[I(I+1)-\tfrac{1}{4}]\,\frac{1}{5} S(S+1) \times \gamma_I^2\, \gamma_S^2\, \hbar^2\, r^{-6}\, e^{-i\omega_o t}\, e^{-t/\tau_c}$$

Substituting these correlation functions in equation (3.34) and equation (3.32), the values of T_1 and T_2 were obtained numerically. Figs. (2.2 and 2.3) show T_1 and T_2 versus $1/T$ for Li_5AlO_4 where solid lines are the theoretical fit using the following data

$r = 2.5$Å, $S = 5/2$ for Fe^{3+}, $\gamma_S = 1.76 \times 10^7\ \mathrm{oe}^{-1}\ \mathrm{sec}^{-1}$, $\gamma_I = 1.04 \times 10^4\ \mathrm{oe}^{-1}\ \mathrm{sec}^{-1}$, $\nu_o = 1.6 \times 10^{13}\ \mathrm{sec}^{-1}$, $E_a = 0.96$ ev obtained from the conduc-

tivity data. The concentration of impurities c was taken to be 350 ppm instead of the EPR value of 150 ppm in order to make the theoretical T_1min agree with the experimental value.

The fit between the theory and experiment seems reasonable, but one deficiency in this exercise is the possibility of some quadrupolar effects playing a role. The procedure which we adopted in treating nuclei having a quadrupole moment, is to subtract T_1^{-1} impure from T_1^{-1} pure and relate the difference to the effect of the paramagnetic ions. Unfortunately this was not possible for Richards' due to the lack of the variation of the level of the paramagnetic ions.

O. Abou et al (1982) succeeded in simplifying the rate equations due to Richards' (1978). These equations have a simple form and can be used without the need for substantial numerical work, hence simply allow appreciation of the effect of paramagnetic ions on the relaxation rates. This model although simple does not have the versatility of that of Richards', since it deals with the general case of the transferred hyperfine interaction. The model assumes that the diffusing ions need not feel a continuous range of local fields but only a few should be sufficient, especially when dealing with fast ion conductors. Assuming three types of local fields; zero and $\pm\ \delta/\gamma$ referred to as [1], [2] and [3]. When the diffusing ion is far from the impurity, local field [1] is assumed, [2] and [3] refer to spin up and down respectively. δ is the interaction strength which is taken as the transferred hyperfine constant and γ is the nuclear gyromagnetic ratio.

(a) The Effect of Paramagnetic Ions on T_2

The correlation function is given (Abragam (1961)) as

$$G(\omega,\nu_c) = \frac{1}{n(1+n)} \mathrm{Re}\,[1 \quad \tfrac{1}{2}n \quad \tfrac{1}{2}n][M]^{-1} \begin{vmatrix} 1 \\ 1 \\ 1 \end{vmatrix} \qquad (2.36)$$

where M is a matrix of the form

$$M = \begin{vmatrix} i\omega - n\nu_c & \frac{1}{2}n\nu_c & \frac{1}{2}n\nu_c \\ \nu_c & -i(\omega-\delta)-\nu_c & 0 \\ \nu_c & 0 & -i(\omega+\delta)-\nu_c \end{vmatrix}$$

In this matrix the off-diagonal element represent the probability of transition between the three kinds of sites. The value of n is zc and ν_c is the hopping rate of the mobile ion. If interaction between the paramagnetic ions is included in the formalism, it has the effect of inverting the spins, converting a type [2] site to type [3] site and vice versa, the matrix M becomes.

$$M = \begin{vmatrix} i\omega - n\nu_c & \frac{1}{2}n\nu_c & \frac{1}{2}n\nu_c \\ \nu_c & -i(\omega-\delta)-\nu_c\nu_s & \nu_s \\ \nu_c & \nu_s & -i(\omega+\sigma)-\nu_c-\nu_s \end{vmatrix}$$

where ν_s is the hopping rate of the paramagnetic ion, the correlation function of equation (3.36) leads to a spin spin relaxation rate of the form

$$T_2^{-1} = \frac{n\delta^2\nu_c}{\nu_c^2+\delta^2 + 2\nu_c\nu_s} \qquad (2.37)$$

Equation (2.37) has a low temperature limit of n/τ_c and a high temperature limit of $n\delta^2\tau_c$ which correspond to the equations obtained by Hogg et al (1977) and used to interpret his data on PbF_2 doped with Mn^{2+}.

(b) The Spin lattice relaxation time due to paramagnetic ions

In general the field produced at the site of the paramagnetic ion is not parallel to the external field. The angle between the two fields is taken as θ and the resultant of the fields is called B_2. If a diffused nucleus of magnetic moment m_o enters from site [1] to site [2], it will precess about the field B_2 according to

$$m(t) = m(o)[\cos^2\theta + \sin^2\theta \cos(\gamma B_2 t)].$$

The mean life time in site [2] is ν_c^{-1} so the average change for a single visit to this site is

$$= -\sin^2\theta\, m(o) \int_o^t [1 - \cos(\gamma B_2 t')]\, \exp(-\nu_c t')dt' / \int_o^\infty \exp(-\nu_c t')dt'$$

$$= -m(o) \sin^2\theta \frac{\omega_2^2}{\omega_2^2 + \nu_c^2}$$

where $\omega_2 = \gamma B_2$, the jump will occur at a rate of $\frac{1}{2}n\nu_c$ so the rate of change of magnetization parallel to the applied field is

$$\frac{dM}{dt} = - M \sin^2\theta \frac{n\nu_c}{2} \frac{\omega_2^2}{\omega_2^2 + \nu_c^2},$$

Jumps to a site of type [3] produce a similar term, hence adding them, we get for the spin lattice relaxation rate

$$T_1^{-1} = n\, \nu_c \sin^2\theta \frac{\omega_2^2}{\omega_2^2 + \nu_c^2} \qquad (2.38)$$

Equation (2.38) has a simpler form when the local field is much smaller than the applied field, giving a result similar to those obtained through the application of perturbation theory.

$$T_1^{-1} = \frac{n\nu_c}{\nu_c^2 + \omega_o^2} \delta^2 \qquad (2.39)$$

Equations (2.37 and (2.39) used to fit the data of PbF_2 doped with Mn^{2+} obtained by Hogg et al (1977). The fit showed a good agreement between the theory and the experiment. The crucial test for the theory was thought to interpret data for nuclei with a quadrupole moment. The study was to investigate $Li_{0.5}\ Y_{0.5}\ Zr\ S_2$ which is a lithium ion conductor. This material was doped with 1% Cr^{3+} which is expected to replace some of Y^{3+}. In order to fit the data of T_1 and T_2 due to paramagnetic ions, the part of the relaxation which could come for example from quadrupolar effects was removed. The procedure was to subtract T_1^{-1} and T_2^{-1} data obtained for the doped sample from T_1^{-1} and T_2^{-1} of the undoped sample, hence the data could only be related to the effect of the paramagnetic ions. The parameters used in the fitting procedure were C =

0.0007, the hyperfine constant $\delta = 2 \times 10^7$ Hz, the electron relaxation time $\tau_e = 5 \times 10^{-7}$ sec, the attempt frequency $\nu_o = 3.4 \times 10^{10}$ sec^{-1} and the activation energy = 0.18 ev. Fig. (2.4) shows T_1^{-1} at three different frequencies of 29.8, 22.3, 15.3 MHz and T_2^{-1} at 29.8 MHz while the solid lines are the theoretical fits using equations (2.37) and (2.39). The good agreement between the theory and experiment supports the notion that magnetic tagging techniques can be used successfully in materials with spin > $\frac{1}{2}$, especially lithium and sodium fast ion conductors which are very promising materials to use in practical applications.

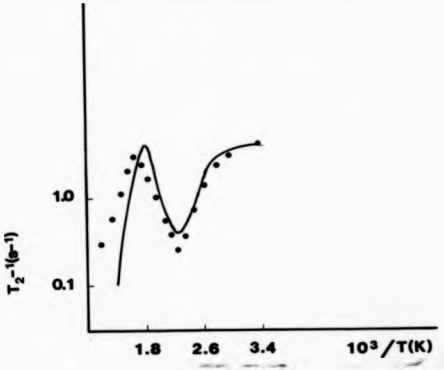

Fig.2.1 T_2^{-1} of Mn doped PbF_2. (•) After data of Hogg et al (1977). Curve is theory with parameters given in the text (Richards 1978).

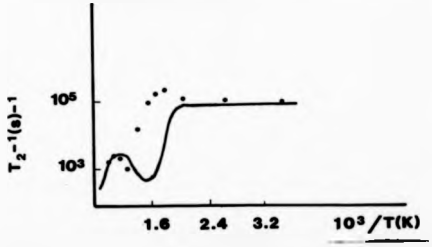

Fig.2.2 T_2^{-1} of Li_3AlO_3(•)After data of Follstaedt et al (1978). Curve is theory with parameters given in the text (Richards 1978).

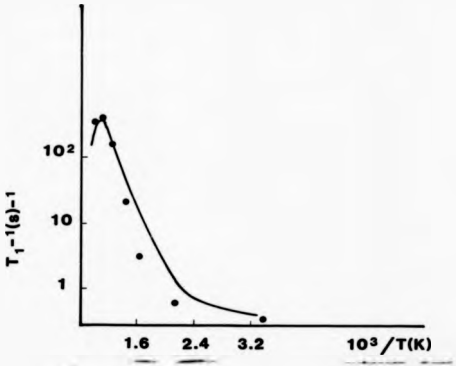

Fig.2.3 T_1^{-1} Li_5AlO_4. (•) are data of Follstaedt et al (1978). Curve is theory with parameters given in the text Richards (1978).

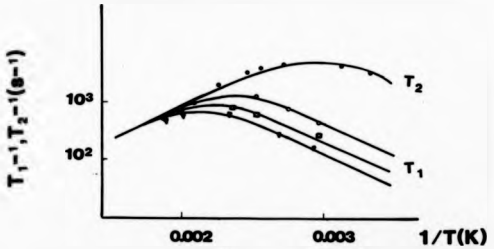

Fig.2.4 The contribution to T_1^{-1} and T_2^{-1} due to paramagnetic impurities in doped $LiYZrS_2$. The solid lines are theoretical fit (O.Abou et al 1982).

CHAPTER THREE

EXPERIMENTAL

3.1 Sample Preparation

3.1.1 Lithium - Titanium Oxides

(a) $Li_2Ti_3O_7$

This compound was prepared as described by Izquierdo et al (1980). An amount of Li_2CO_3 and TiO_2 were mixed according to the chemical reaction as,

$$Li_2CO_3 + 3\ TiO_2 \rightarrow Li_2\ Ti_3O_7 + CO_2$$

The chemicals were supplied by Johnson and Matthey chemicals, with high purity of 99.999%. The weighed constituents were mixed into a paste with acetone and the mixture was heated in a platinum crucible at 600°C for two hours in order to liberate CO_2, and finally at 1200°C for two days to complete the reaction. It was rapidly cooled to room temperature to prevent decomposition. This material has an orange colour as reported in the literature Morosin et al (1979). The constituents were ground to a fine powder then sealed under vacuum in a silica tube of 1 cm diameter.

In the case of the off-stoichiometric $Li_2Ti_3O_7$, a sample with lithium excess was prepared. This was done by adding 1% by weight of Li_2CO_3 to the constituents for making stoichiometric $Li_2Ti_3O_7$. A structural investigation using X-rays did not reveal much change from the stoichiometric sample. This is obvious since a small increase of lithium will have little effect, because X-ray scattering is influenced more by the titanium.

(b) Li_2TiO_3

In preparing Li_2TiO_3, the same high purity Li_2CO_3 and TiO_2 were used

in proportions according to the chemical formula,

$$Li_2CO_3 + TiO_2 \rightarrow Li_2TiO_3 + CO_2$$

The constituents were mixed and heated at 1000°C in a platinum crucible for five days following a procedure reported by Huggins et al (1973).

To check that the samples of $Li_2Ti_3O_7$ and Li_2TiO_3 prepared in this way have the same structures as those reported in the literature, X-ray spectra were taken for both samples and compared with the spectra computed from the structural parameters obtained by Izquierdo et al (1980) and Huggins et al (1973) tables (3.1) and (3.2) The agreement was excellent.

3.1.2 The Lisicon System

In the lisicon system two samples were prepared

i) $Li_{12}Zn_2(SiO_4)_4$

ii) $Li_{12}Mg_2(SiO_4)_4$

To prepare the above materials a mixture of Li_2CO_3, MgO or ZnO and SiO_2 with purity of 99% were placed in an alumina crucible and reacted by firing overnight in air at a temperature of 1100°C as described by Hong (1978). These samples were dried under vacuum at a temperature of 200°C for two days to ensure the removal of any vapour, then sealed in silica glass tubes of diameter 1 cm, ready for insertion in the nmr probe.

The structures of the samples $Li_{12}Zn_2(SiO_4)_4$ and $Li_{12}Mg_2(SiO_4)_4$ have been determined from x-ray powder diffraction patterns using the Hesse-Lipson procedure described by Azaroff (1968). The samples were found to be orthorhombic with the values of the lattice parameters very close to those found by Hong (1978) for $Li_{14}Zn(GeO_4)_4$.

3.2 The NMR Spectrometer

The nuclear magnetic resonance work performed in this thesis was carried out using a spectrometer constructed in the department of physics with facilities appropriate for studying solid state substances. It

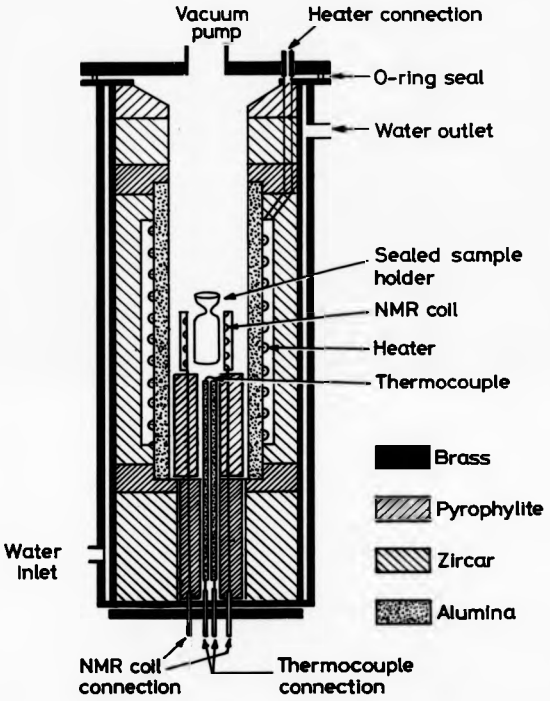

Fig.3.1 NMR Furnace.

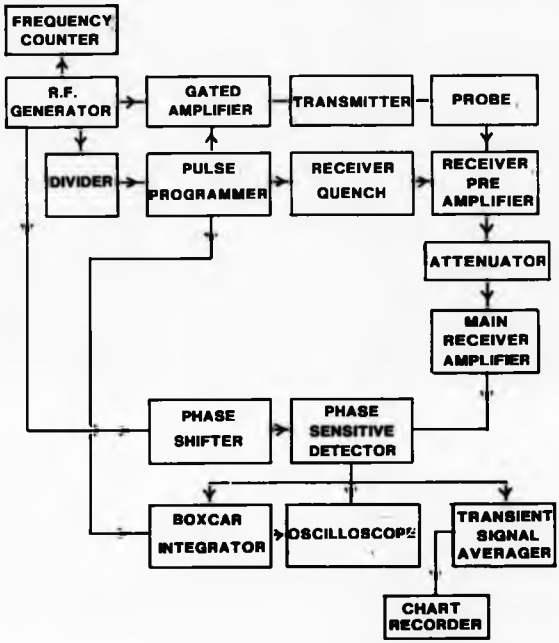

Fig.3.2 Block diagram of the NMR pulsed spectrometer.

consists of the following parts fig. (3.2).

probe, magnet, transmitter, receiver and the detection system.

3.2.1 The sample probe

The probe is shown in fig. (3.1) and was made of brass in the shape of a hollow cylinder of length 25 cm and diameter 4 cm. This size is appropriate for the pole gap of the magnet. The concentric brass furnace tubes have a spacing of about 0.5 mm to provide water jacket. The heater winding of Nichrome surrounds the sample and is capable of providing temperatures up to 800°C. A thermocouple made of nickel-chromium/nickel-aluminium was fitted to touch the bottom of the tube containing the sample and connected to a Thor Cryogenic Model 3010 temperature controller which is stable to $\pm$ 2°C. The probe is filled with argon since the coil material reacts with oxygen at high temperature. The coil was made up of molybdenum wire having 15 to 16 turns in a length of 2 cm with a diameter of 1.1 cm. A single coil was used for the transmitter and the receiver system instead of having a separate coil for each. This configuration has some advantages especially as it is easy to accommodate a single coil in the space available. One can avoid some mechanical vibrations and the single coil is less susceptible to temperature drift. The generation of the B_1 r.f. field within the volume of the sample can be expressed as Clark (1964),

$$B_1 = \frac{3PQ}{\omega_0 V}$$

where P is the transmitter pulse power in watts

Q is the quality factor of the resonant circuit

ω_0 is the resonance frequency in MHz

V is the coil volume in cm^3

The coil was designed such that the ratio of the sample volume to the coil volume as approximately unity. The Q value was defined as

$$Q = \frac{\omega_o L}{R}$$

where L and R are the inductance and the resistance of the coil. It is advantageous to have a high value Q, which can be achieved by having high L or low R values. This large Q value gives a higher signal to noise ratio but makes the recovery time longer.

After assembling the parts of the probe, an important procedure is to tune it. The aim of this action is to ensure that the output of the transmitter is properly dissipated into the sample and the NMR signal amplified by the receiver. These conditions can be achieved by the circuit of fig. (3.3), which contains the coil represented by the inductance L and two variable capacitances C_1 and C_2. The change of the capacitance C_1, will change the resonant frequency of the circuit and ultimately make the circuit resonate with the same frequency as the nuclei, this is known as tuning. Another important action for the circuit is to make the impedance of the probe the same as the coaxial cable connected to the transmitter which is 50 Ω. This can be achieved by varying the capacitance C_2. This procedure is known as the matching process. To select the values of C_1 and C_2 a hybrid tee is used which contains four ports. One of the ports is used to connect to an rf sweep generator and one is connected to a measuring device e.g. oscilloscope. The remaining two are connected to the probe and to a known impedance usually a 50Ω load. The signal generator generates a signal of previously set frequency. The impedance of the probe is varied by varying the capacitors to match that of the known load. When the impedance of the probe matches that of the known load, the output from the test connection goes to zero and the probe is said to be matched.

The circuit of fig. (3.3) represents the capacitor configuration used in the probe and also shows the connection with the transmitter and

receiver used to effect isolation. During the application of the rf pulse both the crossed diodes D_1 and D_2 are conducting heavily and have low impedances. The receiver is protected from this large voltage because D_2 isolates the receiver from the transmitter. This relies on the transformation properties of $\lambda/4$ cable and the non-linear characteristics of diodes (Lowe et al 1968). Following the rf peak maximum D_1 and D_2 will be open circuited and the weak NMR signal passes to the preamplifier.

3.2.2 The Magnet

The magnet provided for the experiment is a water cooled electromagnet having a power supply both supplied by Newport instruments. Also the magnet is fitted with a field controller unit type Bruker B-HUD to vary the magnetic field. This magnet is capable of providing a field up to about 20KG. In this experiment the highest field needed was about 13 KG when a Larmor frequency of 21.5 MHz was used. The magnet has a pole face gap of 4.5 cm and is provided with a Hall probe to determine the field.

3.2.3 The transmitter

The transmitter consists of a crystal generator capable of providing frequencies of 7.5, 12.3 and 21.5 MHz. This generator delivers a power of about 1 kw into a 50 Ω load, a requirement for use in solid state NMR. Also its rise and fall time is much smaller than the pulse length, which in the case of ^7Li is about 4 μs for a 90° pulse. The radio frequency signal is divided into three outlets. One is used as a reference for the phase sensitive detector and the other two are fed to two phase shifters outputs of which pass through gates driven by the pulse programmer. The pulse generation is accomplished with a programmer built in the Department of Physics which provides a range of pulses with spacing from 1 μs to

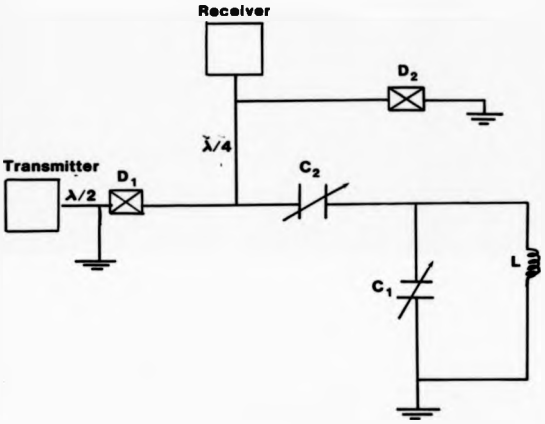

Fig.3.3 Transmitter-receiver isolation network and probe capacitor configuration.

1 sec. and with a pulse repetition frequency from 200 μ sec to 10 sec. The outputs of the gates are contained and fed into a chain of amplifiers which are finally conencted to the probe via a coaxial cable of length $\lambda/2$. A power supply giving up to 2kV is provided for the high power amplifiers.

3.2.4 The Receiver and the Detection System

The output signal from the receiver/transmitter probe is fed to the preamplifier and via $\lambda/4$ coaxial cable to the receiver. The receiver consists of an amplifier to bring the signal to the level to be detected by the oscilloscope, and a phase sensitive detector which integrates the nmr signal with the reference one. The free induction decay obtained through the receiver system is fed to a Bruker TMC-600 averager with 2k word memory and time resolution of 50 ns/word. The signal is accummulated N times and with the use of the averager one gets $N^{\frac{1}{2}}$ improvement in the signal to noise ratio. The output of the averager is either fed to an oscilloscope or plotted on a y-t recorder for analysis.

3.3 Measurements of the Relaxation Times

To describe the effect of a pulse on the spin system it will be appropriate to use a rotating frame of reference with coordinates x', y', z' in which z' coincides with the z axis of the laboratory frame and the x' y' plane is rotating at the Larmor frequency. If we apply rf radiation we disturb the magnetisation from its equilibrium, assuming it is in the z' direction. The magnetization moves away from the equilibrium position making an angle θ with the z' axis fig. (3.4). This angle depends on the duration of the radiation τ_w. Two cases are of practical importance.

(a) When $\theta = \pi/2$, in this case we have

$$\tau_w \gamma B_1 = \pi/2 \qquad \text{or } \tau_w = \pi/2\gamma B_1$$

the magnetization after the 90^0 pulse will lie in the y' axis.

(b) when $\theta = \pi$

then $\tau_\omega \gamma B_1 = \pi$ or $\tau_\omega = \pi/\gamma B_1$,

The 180° pulse is twice as long as the 90° pulse and its effect is to invert the magnetization into - z' direction. It is important that the pulse must be short so that no relaxation processes occur during the pulse.

3.3.1 Free Induction Decay

Assuming the spin assembly is by a 90° pulse, this will tip the excited equilibrium magnetization M from the z' axis into the y' axis. Since each part of the spin system experiences different local fields which could be related to magnetic field inhomogeneity, dipolar interaction, etc. then some spins will resonate with frequency greater than the Larmor frequency and some with lower frequency. These groups of spins are called isochromats which rotate clockwise and anticlockwise relative to the centre isochromat resulting in a dephasing process leading to the decay of magnetization known as free induction decay fig. (3.5). If the field inhomogenity is the main source of destroying the magnetisation in x'y' plane, then the observed time constant T_m is

$$\frac{1}{T_2^*} = \frac{1}{T_2} + \frac{1}{T_m}$$

where $1/T_m$ is due to inhomogenity dephasing and T_2 is the transverse relaxation time.

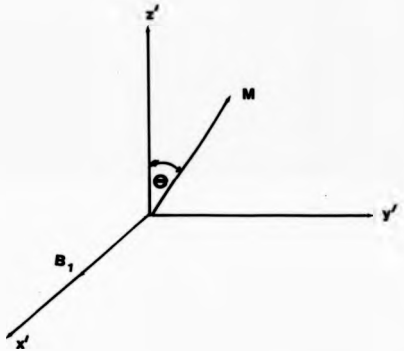

Fig.3.4 On resonance rotation of the magnetization vector in the rotating frame. The angle swept, $\theta=\gamma B_1 \tau$

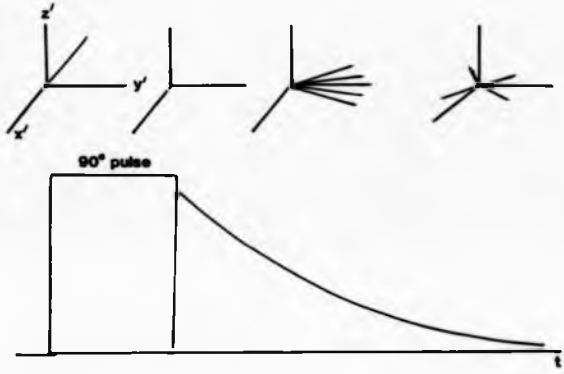

Fig.3.5 Behaviour of spin isochromats following a 90° pulse.

3.3.2 The Saturation Recovery Method

A few sequences for measuring T_1 will be reviewed, the first is the saturation recovery or $90°-\tau-90°$ pulse sequences. Following the first $90°$ pulse which tips the magnetization into the y' direction a second pulse is applied after time τ, which has the effect of turning the magnetization M_z into the x'y' plane and a free induction decay is observed. The z-component of the magnetization is

$$M_z = M_o\ (1 - \exp - \tau/T_1)$$

or

$$\frac{M_o - M_z}{M_o} \exp\ (-\tau/T_1) \qquad (3.1)$$

by varying the waiting time τ, different values of M_z are obtained. It is very important to accurately measure the equilibrium magnetization M_o which can be achieved by making τ very long and observing the constancy of its value by going to a longer delay time. It is possible that M_o changes during the experiment hence it will be preferable to measure M_o for every other measurement of M_z. Plotting M_o-M_z versus τ on a semilog scale yield a straight line and from the slope a value of T_1 is obtained.

3.3.3 The Inversion Recovery Method

This sequence is known as the inversion recovery or $180°-\tau-90°$ pulse sequence. It is very popular for measuring T_1, especially when it is not very long. Relaxation times measured here never exceeded a few hundred millisecond. The essence of the sequence is that by applying $180°$ pulse, the magnetization is inverted taking the -z direction. The final equilibrium value is reached by M_z decreasing in magnitude passing through zero and growing in the z-direction with a time constant T_1. Another pulse of $90°$ will tip M_z into x'y' plane and a free induction decay will be a measure for M_z. The z-component of magnetization varies with time according to

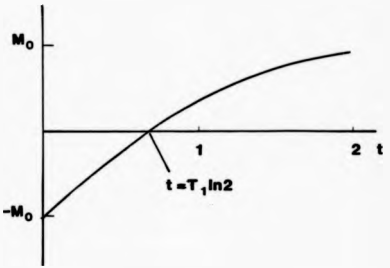

Fig.3.6 Range of magnetization in 180°-τ-90° pulse sequence.

$$M_z = M_o (1 - 2\exp - \tau/T_1), \qquad (3.2)$$

M_z passes through zero at $\tau = T_1 \ln 2$, if 180° completely inverts M_o this gives a quick way to get some estimate of T_1. Equation (3.2) is written as

$$\frac{M_o - M_z}{2M_o} = \exp\left(-\frac{\tau}{T_1}\right)$$

Therefore different values of M_z are obtained by varying the delay time. Plotting $M_o - M_z$ versus τ on a semilog scale yields a straight line and from the slope T_1 is obtained. It is also very important to estimate M_o accurately since it would not help taking a large data set for M_z if M_o is not accurate. M_o was measured for other M_z value in these experiments which enabled me to reproduce my data for T_1 with an error not exceeding ± 10%. Another precaution when using this sequence is to wait at least $5T_1$ between each pulse sequence to make sure that the magnetization is at the z direction at the start of each sequence. The dynamic range of magnetization in this sequence is 2 M_o (fig. (3.6)) whereas in the case of 90°-τ-90° it is only M_o. Also in the saturation recovery seqence can be repeated with only a short delay between sequences since the z-component of the magnetization is zero after the 90° pulse regardless of the state of the magnetization before the pulse, hence nothing is gained by waiting between the pulses. This is not valid for the inversion recovery as indicated earlier.

3.3.4 Spin Echo

Hahn's (1950) spin echo method for measuring spin spin relaxation time T_2 is used throughout the measurements. It is valid when T_2 is fairly short, about a few milliseconds. This method is based on applying

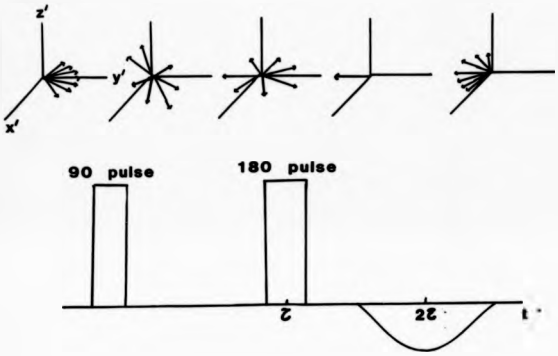

Fig.3.7 The formation of spin echo.

the following 90°-τ-180° pulse sequences. The 90° pulse applied in the x'-axis turns the magnetization into y' axis. The spin isochromats start dephasing in the x'y' plane. At a time τ from the first pulse a 180° pulse is applied which tips the spin isochromats to the other side of x'y' plane. Since the isochromats precess differently as explained earlier, therefore the slower ones are in front and the faster ones are behind so they will move together again and reach a maximum magnetization at time 2τ after the 180° refocussing pulse fig. (3.7). The echo obtained has a height which varies with τ as

$$A_{2\tau} \sim e^{-2\tau/T_2}$$

Plotting the echo's height versus 2τ on a semi log scale gives a straight line and the value of T_2 is obtained from the slope.

TABLE (3.1)

$Li_2Ti_3O_7$

d (spacing) Å	I (relative intensity)
4.4334	100
3.4562	8
2.6859	5
2.5073	28
2.4536	24
2.2416	47
2.1537	5
1.9859	7
1.9688	22
1.8544	9
1.7736	5
1.7295	34
1.6376	21
1.5261	10
1.4719	13
1.4537	5
1.4371	16
1.3993	17

TABLE (3.2)

Li_2TiO_3

d (spacing) Å	I (relative intensity)
4.789	71
4.342	28
4.001	16
3.735	6
2.992	6
2.482	52
2.394	3
2.307	5
2.062	100
1.895	15
1.810	4
1.596	29
1.466	83
1.399	17
1.262	4
1.200	14
1.95	19
1.162	11

CHAPTER FOUR

Li_2O - TiO_2 System

4.1.1 Dilithium Trititanate $Li_2Ti_3O_7$

Johnson W.J. (1964) reported that the introduction of lithium into TiO_2 increases the mobility of lithium and also increases the electronic conduction to a value near that of a semi-metal. There are intermediate phases of LiTiO that might provide high ionic conductivity with low electronic conductivity, which will be suitable as electrolyte materials. These phases exist in a variety of crystalline modification (Huggins (1973)) and as shown in fig. (4.1a).

$Li_2Ti_3O_7$ with a ramsdellite structure, has tunnels of appreciable size which makes it a good candidate for fast ion conduction. It crystallizes in space group Pbmn Lundberg et al (1964), having lattice parameters as a = 5.016Å, b = 9.543Å and c = 2.945Å. The TiO_6 octahedra form a double chain, one octahedron by two octahedra in cross section parallel to c-axis, fig. (4.1). A structural formula of the form $(Li_{1.72}\ \Delta_{2.28})\ (Li_{0.57}\ Ti_{3.43})O_8$ was adopted by Morosin et al (1979), where Δ are vacancies. The first bracket forms the channel site and it is partially filled by lithium ions. The second bracket forms the monochannel site and since there are insufficient titanium ions to fill this octahedral site, it is partially occupied by lithium ions.

The structural considerations indicate the possibility of $Li_2Ti_3O_7$ being a fast ion conductor. Boyce et al (1979) carried out conductivity measurement on a single crystal and on polycrystalline samples using the complex impedance method at various temperatures up to 500°C. The value of the ionic conductivity found at 200°C was $2.6 \times 10^{-3}\ (\Omega\ cm)^{-1}$ which

allows $Li_2Ti_3O_7$ to be classified as a fast ion conductor. The electronic transference number was determined to be $< 10^{-3}$ hence the compound is considered an ionic conductor. Fig. (4.2) shows log σT versus $1/T$, while the values of the activation energies and the prefactors for conductivity along the three crystallographic directions and for the polycrystalline material are given in table (4.1). The variation of the conductivity along different crystallographic directions allows an estimate for the anisotropy which was found,

$$\frac{\sigma_c}{\sigma_b} = 7 \text{ and } \frac{\sigma_b}{\sigma_a} = 4$$

These anisotropy values show that $Li_2Ti_3O_7$ cannot be thought as a completely one dimensional ionic conductor.

4.1.2 Previous NMR work on $Li_2Ti_3O_7$

$Li_2Ti_3O_7$ was first investigated by Huberman et al (1978). They measured T_1 at three different frequencies (8.5, 16.0 and 23.5 MHz), and T_2 at 23.5 MHz in the temperature range 20°C to 500°C. From the experimental curve of fig. (4.3) they concluded

(i) T_1 is Larmor frequency independent, a non BPP behaviour. A few other fast ion conductors also show this behaviour (Follstaedt et al (1976)).

(ii) The activation energy found from T_1 and from the motional narrowing region of T_2 was 0.2ev whilst conductivity gives 0.4ev.

(iii) Above 150°C, T_1 was proportional to T_2, this behaviour was also observed by the authors in CuI which is also a fast ion conductor. They assumed therefore that T_1 was governed by quadrupolar interactions and T_2 by dipolar interactions which led them to write

$$T_2^{-1} = T_2^{-1}|_{dip} + \alpha T_1^{-1} \qquad (4.1)$$

with $\alpha = (I + \frac{1}{2})^2 = 4$, I being the spin of ^7Li

(iv) Due to the lack of frequency dependence of T_1, it was not possible

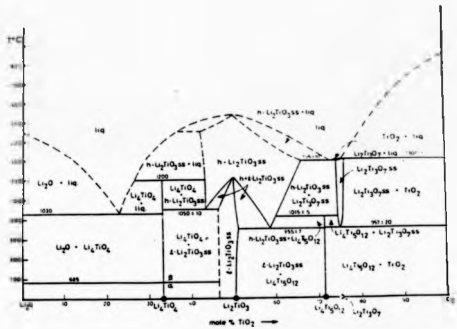

Fig.4.1a The Phase Diagram Li_2O-TiO_2

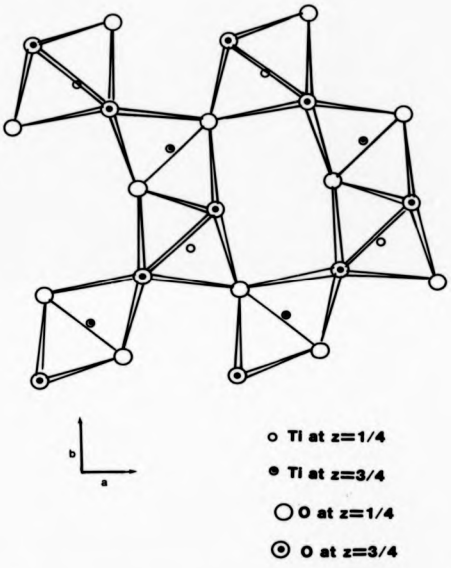

Fig.4.1 The ramsdellite crystal structure of $Li_2Ti_3O_7$.

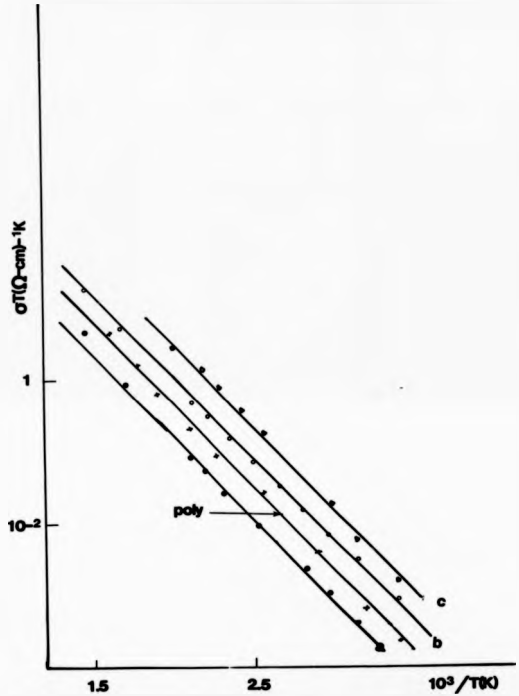

Fig.4.2 The ionic conductivity time temperature versus inverse temperature for polycrystalline $Li_2Tl_3O_7$ and along the three crystallographic directions in a single crystal.

TABLE (4.1)

Activation energy Ea and the prefactor σ_o for $Li_2Ti_3O_7$ from conductivity measurements Boyce et al (1979).

	Ea eV	σ_o $(\Omega cm)^{-1}K$
a-axis	0.46	7.7×10^3
b-axis	0.44	29.2×10^3
c-axis	0.47	194.4×10^3
polycrystalline	0.46	17.4×10^3

to obtain a value for the attempt frequency from T_1 minimum in which the relation $\omega_o\tau_c \sim 1$ holds. Below room temperature T_2 was nearly temperature independent with a value of 100 μ sec. At the beginning of motional narrowing they have $T_{20} = \tau_c$, where T_{20} is the rigid lattice spin spin relaxation time and τ_c is the correlation time of motion. Since the activation energy was known and the hopping rate follows an Arrhenius relation, the attempt frequency was found to be 4×10^7 sec^{-1}. This value is expected to be comparable to the phonon frequency namely $10^{12} - 10^{13}$ sec^{-1}.

The low value of the attempt frequency of some lithium ion conductors which is obvious from table (1.1), led Huberman et al (1978) to put forward an interpretation implying the breakdown of the absolute rate theory in these solids. In order to compare the attempt frequency obtained through NMR data with the optical phonon frequencies obtained by infrared techniques, a dissipation process for ionic hopping is taken into account, and the hopping rate becomes

$$\nu = \frac{\zeta}{kT} \nu_o \exp - Ea/kT \qquad (4.2)$$

with ζ is the average energy the ion losses in each collision with the crystalline cage. The effect of the term ζ/kT is to scale the prefactor ν_o to a value near that obtained by other techniques. An alternative explanation was given by Richards (1978) who tackled the problem of the anomalously low prefactor and low value of the activation energy from the point of view of the dimensionality of these materials and explains these anomalies without the need for invalidating the absolute rate theory. Richards argues that the material discussed by Huberman and Boyce have channel structures which might give rise to one dimensional ionic motion. For such low dimensional materials the prefactor ν_o and the activation energy are obtained from the relations

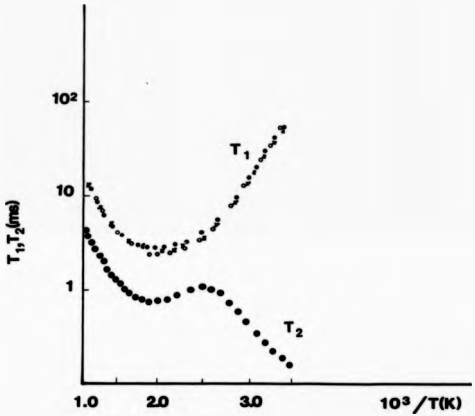

Fig.4.3 T_1 and T_2 as a function of inverse temperature for ^7Li in $Li_2Ti_3O_7$. The T_2 data were obtained at 23.5MHz and T_1 data at 8.5MHz(×), 16MHz(•) and 23.5MHz(•) (Boyce et al 1979).

$$\nu_{eff} = \nu_o \left\{ \frac{<\Omega>^{\frac{1}{2}}}{\nu_o} \right\}^{\frac{4-2d}{4-d}} \quad (4.3)$$

$$E_a' = \left\{ \frac{d}{4-d} \right\} E_a, \quad (4.4)$$

where ν_{eff} is the prefactor obtained from nmr experiment, ν_o is the prefactor which should be comparable with the phonon optical frequency, Ω is the rigid lattice second moment, d is the dimension of the materials and E'_a and E_a are the activation energies measured by nmr and conductivity respectively. To test equations (4.3) and (4.4) on $Li_2Ti_3O_7$ data obtained by Huberman et al (1978), a value of 6.4 x 10^{14} sec^{-1} and 0.6 ev were obtained for the prefactor and the activation energy respectively. Also for β-LiAlSiO the prefactor will have a value of 10^{17} sec^{-1} while the activation energy has a value of 1.2ev. These examples indicate that Richards' equations give unphysical values for both the attempt frequency and the activation energy. Boyce et al (1979) challenged the validity of equations (4.3) and (4.4) in the case of $Li_2Ti_3O_7$. The assumption of it being a one dimensional ionic conductor was not substantiated from the conductivity measurements which gave a small value for the anisotropy Boyce et al (1979). In the case of β $LiAlSiO_4$ the conductivity measurements of Raistrick et al (1976) revealed high anisotropy of about 10^3, which means it can be considered as a one dimensional ionic conductor, nevertheless the values of the prefactor and the activation energy obtained accordingly were unacceptable.

4.1.3 Present Work on the $Li_2Ti_3O_7$

This study investigates both stoichiometric and off stoichiometric $Li_2Ti_3O_7$, measuring the ^7Li spin lattice and the spin spin relaxation times from room temperature up to 350°C for several different frequencies. Three samples were prepared for the stoichiometric $Li_2Ti_3O_7$; two of them were prepared at Warwick and the third one was provided by the University

of York. These samples gave similar results on measuring relaxation times. In the case of the off stoichiometric $Li_2Ti_3O_7$, two samples were prepared with the same Li excess.

Fig. (4.4) shows a plot of T_1 versus 1/T for stoichiometric $Li_2Ti_3O_7$ at three different frequencies of 7.5, 12.3 and 21.5 MHz. The results are summarized as

i) Below the T_1 minimum where $\omega_o \tau_c > 1$, the spin lattice relaxation time T_1 is a frequency dependent, in contrast to Huberman et al (1978), and

$$T_1 \propto \omega_o^{1.0}$$

This dependence is non BPP which would predicts that $T_1 \propto \omega_o^2$. It has been observed that most fast ion conductors follow the relation $T_1 \propto \omega_o^n$, where $n < 2$ and in some cases $n = 0$.

ii) The activation energies obtained from the slope of T_1 below the minimum at different frequencies are the same.

iii) At the T_1 minimum, it was found that,

$$T_{1(min)} \propto \omega_o^{1.0},$$

in accord with the BPP theory.

iv) At high temperature above $T_{1min.}$, the BPP theory assumes that T_1 should be independent of frequency. In fast ion conductors there is a frequency dependence on the dimensionality of the conductor Silbernagel et al (1974) as

$$T_1^{-1} \quad \propto \quad \begin{cases} \omega_o^{-\frac{1}{2}} & 1D \\ \ln \frac{1}{\omega_o \tau_c} & 2D \end{cases} \qquad (4.5)$$

and from the conductivity measurements one cannot classify $Li_2Ti_3O_7$ as a one dimensional conductor. In the region of $\omega_o\tau_c < 1$, T_1^{-1} apparently varies as ω_o^{-1}.

v) At the minimum of the T_1 curve, if $\omega_o\tau_c = 1$ holds and knowing the

activation energy, a value of the attempt frequency was found. It varied between (5-10) x 10^9 sec.$^{-1}$ depending on the frequency. This value is still small compared with the phonon frequency which is in the range of 10^{12} - 10^{13} sec^{-1}. The value of the activation energy plays an important role in determining the attempt frequency. Hence using the value of the activation energy obtained from the motional narrowing region of T_2 and which is comparable with that of the conductivity, then from T_1 minimum, a value of 10^{11} sec.$^{-1}$ is obtained for the attempt frequency. It is still low but over an order of magnitude higher than the previous value.

The T_1 value for the sample prepared at Warwick is about ten times longer than for the sample reported by Huberman et al (1978). A shorter T_1 seems to indicate the existence of paramagnetic ions (the introduction of impurities are often used to reduce the spin lattice relaxation time in materials having long T_1). The anomalous behaviour of the spin spin relaxation time at T > 180°C showing a maximum and a minimum as the temperature changes is also an indication of a role played by paramagnetic ions. This behaviour has been observed in a few fast ion conductors such as PbF_2 doped with Mn^{2+} Hogg et al (1977), $LiYrS_2$ doped with Cr^{3+} O. Abou et al (1982) and Li_5AlO_4 Follstaedt et al (1978). In the cases of PbF_2 and $LiYrS_2$ the paramagnetic ions Mn^{2+} and Cr^{3+} were introduced in a controlled manner and their effect on the relaxation times were studied, while in the case of Li_5AlO_4 it was thought to be very pure but EPR spectra revealed the existence of 150ppm of Fe^{3+} which was causing the relaxation. In the case of $Li_2Ti_3O_7$ the role of paramagnetic ions is different from the previously mentioned cases. Its existence is inherent in the structure, thus a paramagnetic ion in $Li_2Ti_3O_7$ is not an impurity in the sample, but one of its constituents. It seems that a negligible

departure from stoichiometry results in some of Ti^{4+} becoming Ti^{3+} which is paramagnetic. To clarify the stoichiometric effects on the existence of paramagnetic ions, a sample with 1% by weight Li_2CO_3 added to the amount required to prepare the stoichiometric $Li_2Ti_3O_7$. If the Li^+ introduced occupies a site which was originally empty, we need one extra -ve charge to maintain charge neutrality. This could come from Ti^{4+} converting to Ti^{3+}, hence the number of paramagnetic centres is equal to the number of extra lithium ions introduced. Electron paramagnetic resonance measurements of the stoichiometric and off stoichiometric $Li_2Ti_3O_7$ were performed at room temperature and at a frequency of 9.27 GHz. The stoichiometric sample has one small peak while the off stoichiometric sample has three peaks close to g = 2. The spectra of the off stoichiometric sample is an indication of the higher level of the paramagnetic ions.

Fig. (4.5) shows the measured T_1 for the stoichiometric $Li_2Ti_3O_7$ at frequency of 12.3 MHz and for the off stoichiometric sample at two different frequencies of 12.3 and 7.5 MHz as a function of inverse temperature. Values of T_1 for the off stoichiometric material are about ten times shorter than those for the stoichiometric sample, which supports the notion that paramagnetic ions contribute to T_1 in these samples. It was also observed that T_1 values for the off stoichiometric sample were similar to T_1 data obtained by Huberman et al (1978). Below the T_1 minimum the slope of the curve yields an activation energy similar to the value obtained in the case of the stoichiometric sample. T_1 showed a frequency independence in the whole temperature range. This was also observed in the case of $Li_2Ti_3O_7$ investigated by Huberman et al (1978) and $LiAlSiO_4$ studied by Follstaedt et at (1976). This lack of frequency dependence does not allow one to estimate the attempt frequency from T_1

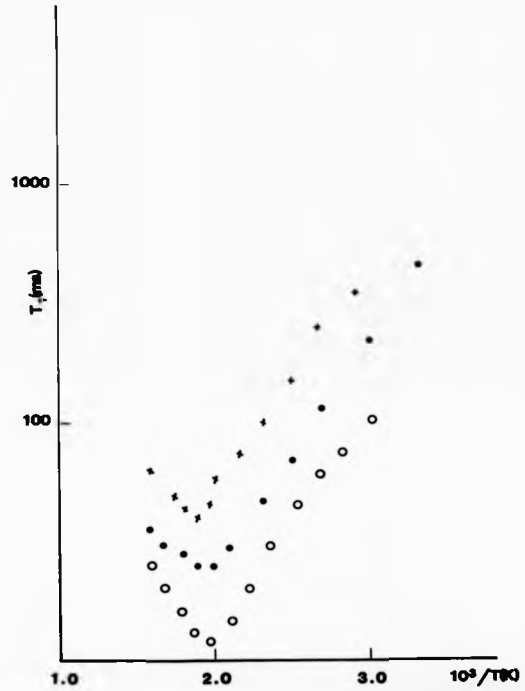

Fig.4.4 T_1 for ^7Li in stoichiometric $Li_2Ti_3O_7$. The data were obtained at 7.5MHz(○), 12.3MHz(•) and 21.5MHz(+).

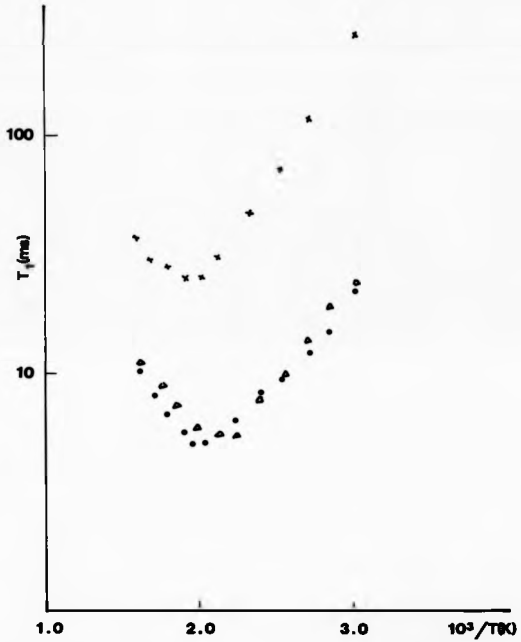

Fig.4.5 T_1(×) for ^7Li in stoichiometric $Li_2Tl_3O_7$ at 12.3MHz. T_1 for ^7Li in the off-stoichiometric $Li_2Tl_3O_7$ where the data was obtained at 12.3 MHz(•) and 7.5MHz(▲).

minimum.

Ionic motion affects the spin-spin relaxation time T_2 and in solids usually $T_2 \neq T_1$, therefore T_1 and T_2 contain different information. Fig. (4.6) shows a plot of T_2 versus $1/T$ for the stoichiometric sample.

(i) As the temperature increases above room temperature and up to 180°C, T_2 starts to increase exponentially due to motional averaging of the dipolar interaction between the lithium ions. In this part of the curve the slope yields a value for the activation energy close to that obtained from the conductivity measurements.

ii) In the high temperature part of the curve $T_1 \neq T_2$ contrary to BPP theory due to motional narrowing. The ratio T_1/T_2 is important in the high temperature region since it gives an indication of the type of relaxation process. When $I > 1/2$ it has been shown that the ratio, (Walstedt (1967)) is

$$\left\{\frac{T_1}{T_2}\right\}_Q = \tfrac{1}{4}\,(I + \tfrac{1}{2})^2$$

and (4.6)

$$\left\{\frac{T_1}{T_2}\right\}_{e-n} = (I + \tfrac{1}{2})^2$$

where Q and e-n indicate that the relaxations to be quadrupolar and paramagnetic. In the case of lithium in which $I = {}^3/_2$, when the ratio is 4 this indicates the relaxation is by paramagnetic ions. From the curve of fig. (4.7) the ratio $T_1/T_2 \sim 2.5$ indicates that paramagnetic ions are probably playing an important role in the relaxation processes.

iii) Approaching room temperature, T_2 looked to be temperature independent with an approximate value of 4×10^{-4} sec. At the start of the motional narrowing $T_{20} = \tau_c$, and using the value obtained for the activation energy, yields a value for the attempt frequency ν_o

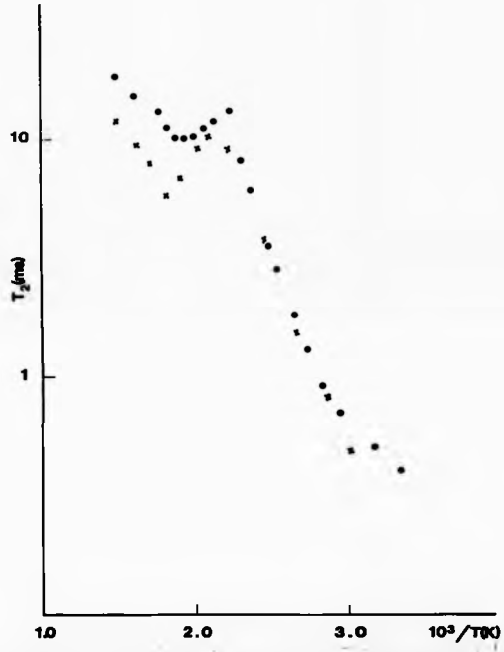

Fig.4.6 T_2 for ^7Li in stoichiometric $Li_2Ti_3O_7$. The data was obtained at 7.5MHz(×) and 12.3MHz(•).

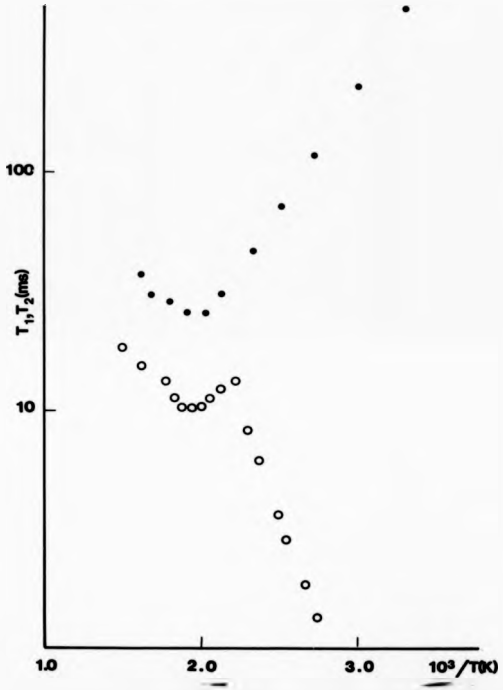

Fig.4.7 T_1(•) and T_2 (○) for ^7Li in stoichiometric $Li_2Ti_3O_7$. The data was obtained at 12.3MHz.

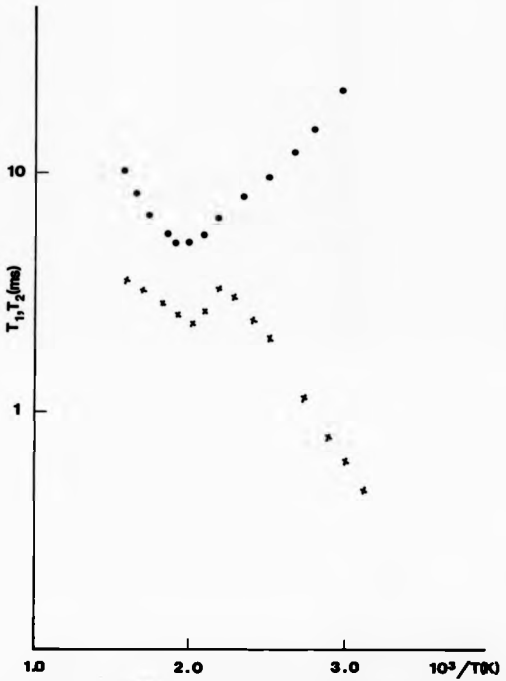

Fig.4.8 T_1(•) and T_2(×) for ^{7}Li in off-stoichiometric $Li_2Tl_3O_7$. The data was obtained at 12.3MHz.

close to that obtained from the T_1 minimum at which $\omega_o \tau_c \sim 1$.

iv) At T > 180°C the curve shows that T_2 first decreases and then increases as the temperature is increased. This temperature behaviour of T_2 is a sign of relaxation by paramagnetic ions.

v) The low temperature part of T_2 as shown in fig. (4.6) is frequency independent as predicted by the BPP theory. Above 180°C, the dependence shown is presumably due to paramagnetic ions.

The T_2 versus 1/T for the off stoichiometric sample shows the same trend as in the case of the stoichiometric fig. (4.8). As the temperature increases from room temperature up to 180°C, T_2 increases exponentially with the increase of temperature. The slope of the curve yields an activation energy close to that obtained from T_1 for both stoichiometric and off stoichiometric samples. This activation energy is smaller than that obtained from T_2 for the stoichiometric sample and from the conductivity measurements, as shown in table (4.2) which gives the dynamical parameters obtained from both stoichiometric and off stoichiometric $Li_2Ti_3O_7$. On the onset of motional narrowing $T_{2o} \sim \tau_c$, and with the use of activation energy obtained from the slope, the attempt frequency was found to be about 10^7 sec.$^{-1}$ which is similar to that obtained by Huberman et al (1978).

4.1.4 Magnetic Contribution to Relaxation Rates

(i) Transferred hyperfine interaction

In analysing the experimental relaxation rates of the stoichiometric and off stoichiometric $Li_2Ti_3O_7$, use of a theory developed by Richards (1978) and later simplified by O Abou et al (1982) is applied extensively. These equations were discussed in Chapter two. This theory was very successful in accounting for the magnetic tagging technique especially in the case of $Mn:PbF_2$. The reason for that is the fact that fluorine ion

has a spin $\frac{1}{2}$ and has no quadrupole moment to affect relaxation processes. The structure of PbF_2 is simple and the contact interaction which determines the relaxation rates is accurately known from EPR experiments. In the case of lithium ion which has a spin $^3/_2$, the magnetic and quadrupolar processes effect the relaxation mechanism. Motional narrowing collapses the quadrupolar satellite into the central line which results in T_2^{-1} similar to that caused by paramagnetic ions. To remove this quadrupolar effect from the experimental data, a method was applied where the relaxation rates T_1^{-1} and T_2^{-1} of the stoichiometric sample were subtracted from the off stoichiometric sample. This difference is attributed to the effect of the paramagnetic ions.

(a) Spin Lattice Relaxation Time

In the spin lattice relaxation time T_1 one relaxation mechanism is playing a role in the whole temperature range of interest. This relaxation is governed by paramagnetic ions and the rate of T_1 is written as (Chapter two).

$$T_1^{-1} = \frac{zc\delta^2 \tau_c}{1+\omega_o^2 \tau_c^2}, \qquad (2.39)$$

(the terms of the equation (2.39) were explained previously in text). Fig. (4.9) shows T_1 (due to paramagnetic ions) against the inverse of temperature, the solid line is a fit using equation (2.39) with parameters given in table (4.3). The value of the transfer hyperfine constant used is the same as that used in the T_2 fit. To get the concentration of the paramagnetic ions, T_1 obtained from equation (2.39) is scaled to that obtained experimentally, hence a value of c was found. This is the only adjustable parameter, the values of the activation energy and the attempt frequency used in equation (2.39) were obtained from the experimental T_1 curve.

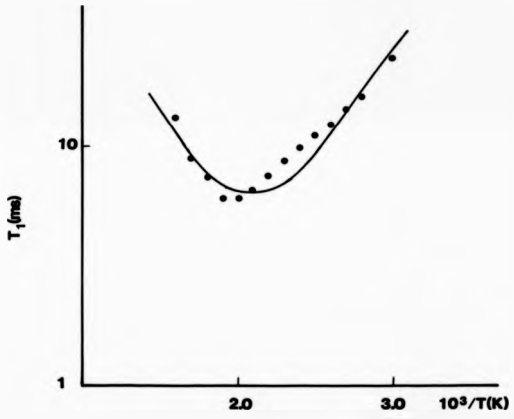

Fig.4.9 The contribution to T_1 due to paramagnetic ions in $Li_2Tl_3O_7$.The solid line obtained using equation (2.39).

TABLE (4.2)

Values of the different dynamical parameters for stoichiometric and off stoichiometric $Li_2Ti_3O_7$ through measurements of T_1 and T_2.

Sample	Activation Energy E_a(ev)	Attempt frequency $\nu_o(sec)^{-1}$	Remarks
Stoichiometric $Li_2Ti_3O_7$	0.2 (T_1)	$(5-10)\times10^9$ (at different frequencies)	T_1 min
	0.4 (T_2)	10^{10}	linewidth
Off stoichiometric $Li_2Ti_3O_7$	0.2 (T_1)		
	0.2 (T_2)	10^7	linewidth

TABLE (4.3)

Activation energy Ea (ev)	0.2
Attempt frequency ν_o $(sec)^{-1}$	10^{10}
Hyperfine constant δ $(sec)^{-1}$	1.1×10^8
Electron Relaxation time τ_e (sec.)	1.2×10^{-6}

To show that the spin lattice relaxation time is not due to dipole dipole coupling between the diffused lithium ions, a plot of T_1 (dipolar) versus 1/T is shown in fig. (4.11). The parameters used in the plot were obtained from the low temperature part of T_2 which is governed by dipolar interactions. These constants were the attempt frequency and the activation energy which have the values of 10^{10} Hz and 0.4eV respectively. According to this model the minimum T_1 occurs at a temperature of about 827°C with a value of T_1 minimum of 1.8×10^3 m sec, while experimentally T_1 minimum occurs at a temperature of about 227°C with a value of 25 m sec. Therefore from the previous data the dipole dipole interaction between the lithium ions cannot account for T_1 relaxation.

(b) Spin-Spin Relaxation Time

In the spin spin relaxation time T_2, the interpretation is based on dividing T_2 versus 1/T into two regions, each region is governed by one type of relaxation process. In region I in which T > 180°C, the relaxation is due to paramagnetic ions, therefore the subtracted data was fitted to a relation of the form (Chapter two),

$$T_2^{-1} = \frac{2c\tau_c\tau_e\delta^2}{\tau_c^2\tau_e\delta^2+\tau_c\tau_e} \qquad (2.37)$$

Fig. (4.10) shows the experimental data for region I taken at a Larmor frequency of 12.3 MHz. The solid line is the theoretical fit using equation (2.37) with parameters given in table (4.3). The criteria for selecting the parameters used in equation (2.37) and tabulated in table (4.3), is to use those obtained experimentally such as the attempt frequency which was found from the relation $\omega_o\tau_c \sim 1$ at T_1 minimum and with the use of the activation energy obtained from the slope of the T_1 curve. This value of the attempt frequency was also obtained from the onset of the motional narrowing region where $T_{2o} = \tau_c$ and was found to be

the same as that obtained from the T_1 minimum. The value of the activation energy used was the same as that obtained from T_1 measurement rather than that obtained from the motional narrowing region of T_2 which is dominated by dipolar coupling. This choice of the activation energy is due to the fact that these regions of T_2 and T_1 are both dominated by paramagnetic relaxation. The transferred hyperfine constant and the electron relaxation time can be obtained from EPR data. A procedure is adopted in selecting these unavailable constants, where T_2 is plotted against the inverse of temperature for different values of transferred hyperfine constants varying from 1.2×10^7 to 1.1×10^8 sec.$^{-1}$. It is clear from fig. (4.12) that changing this constant shifts the minimum of T_2 towards the high tempera- ture region of T_2 versus 1/T curve. The value selected for the constant is the one in which both minima of the experimental and calculated T_2 coincide. For selecting a value of the electron relaxation time, a variation between 1.2×10^{-6} to 1×10^{-8} sec. were used in plotting T_2 as shown in fig. (4.13). The effect of these variations on T_2 was to vary the depth of the minimum. The value selected was 1.2×10^{-6} sec. which gives the best fit to the experimental data.

In region II in which T < 180°C, the relaxation T_2 is due mainly to dipole dipole coupling between the diffusing lithium ions and the effect of the paramagnetic ions in this region is negligible. The rate of T_2 due to dipolar interaction can be written as

$$T_2^{-1} \sim \Omega \tau_c$$

where Ω is the dipolar second moment which has the form

$$\Omega = \frac{2}{5} \gamma^4 \hbar^2 I (I + 1)/r^6$$

where γ is the lithium gyromagnetic ratio, $\hbar$ is Planck's constant, r is the average Li-Li distance and I is the spin which is $^3/_2$ for lithium. The parameters used in equation (2.22) are given in table (4.4). The fit

to the experimental data is in a good agreement as shown in fig. (4.11) and in the high temperature region $T_1 \sim T_2$. Approaching room temperature T_2 is not described by the motional narrowing process rather it is governed by the rigid lattice limit where $T_{20}^{-1} \sim \Omega^2$ in which T_{20}^{-1} is the spin spin relaxation rate found to be about $2.5 \times 10^{+3}$ sec^{-1}, while Ω^2 is calculated as 5×10^3 sec^{-1}, a factor of 2 between the two values. In calculating the second moment the Li-Li distance was taken as 2.9Å given by Morosin et al (1978).

It is clear from tables (4.3) and (4.4) that two activation energies were used in the fitting procedure. These values as was pointed out in the text were obtained experimentally from T_1 and the motional narrowing region of T_2. They cannot be attributed to experimental inconsistency since as indicated the measurements of T_1 and T_2 for the stoichiometric sample were done three times. The difference in the activation energy could be due to the existence of two different sites for Li ions. The channel site which is occupied only by lithium ions and the non channel site which is available for both lithium and titanium. The non channel site is responsible for lithium experiencing the effect of the paramagnetic titanium and due to that the activation energy is different. This effect could be thought of as a short range interaction not contributing to the conductivity. In the channel site which is partially filled, the lithium ions could jump to the available vacancies contributing to the conductivity with an activation energy similar to that obtained from the conductivity measurements.

The good agreement shown in fitting T_1 and T_2 to a relaxation based on the transferred hyperfine is clear. One defect with this exercise is the value found for the impurity concentration was a few ppm. This unrealistic value especially for 1% of excess lithium introduced to the

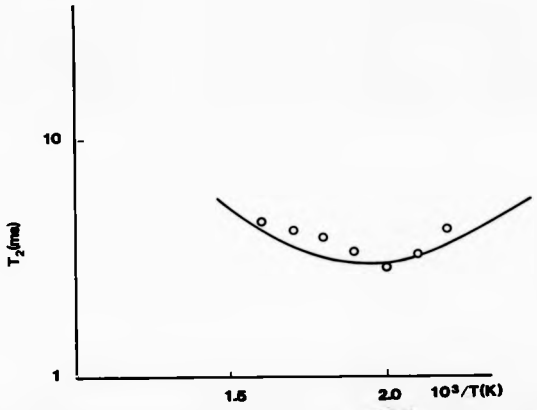

Fig.4.10 The contribution to T_2 due to paramagnetic ions in $Li_2Ti_3O_7$. The solid line obtained using equation (2.37).

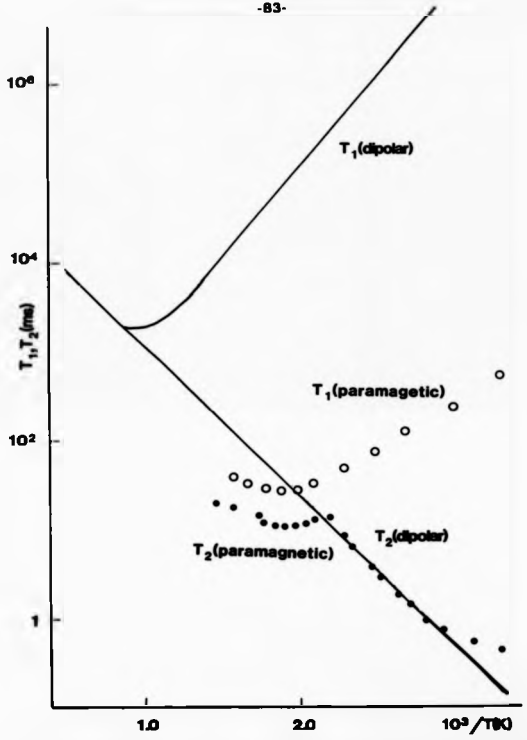

Fig.4.11 Variation of T_1 and T_2 for ^7Li in $Li_2Ti_3O_7$ showing different regions of interaction.

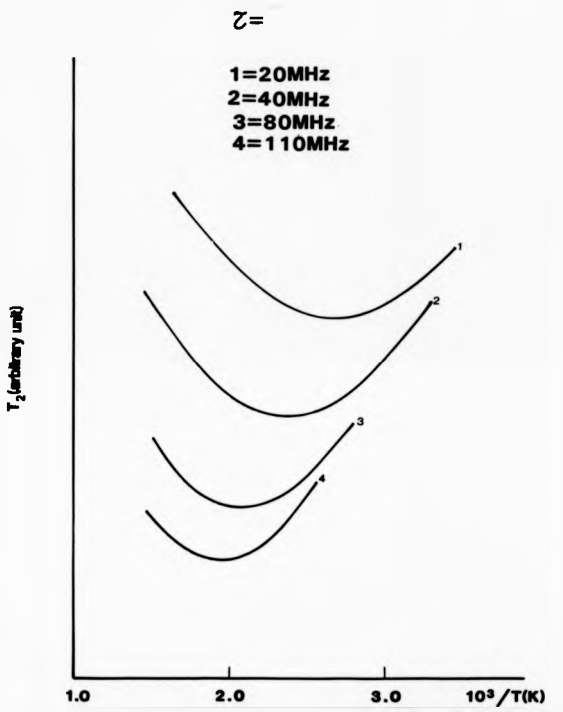

Fig.4.12 T_2 for different values of transfer hyperfine constant.

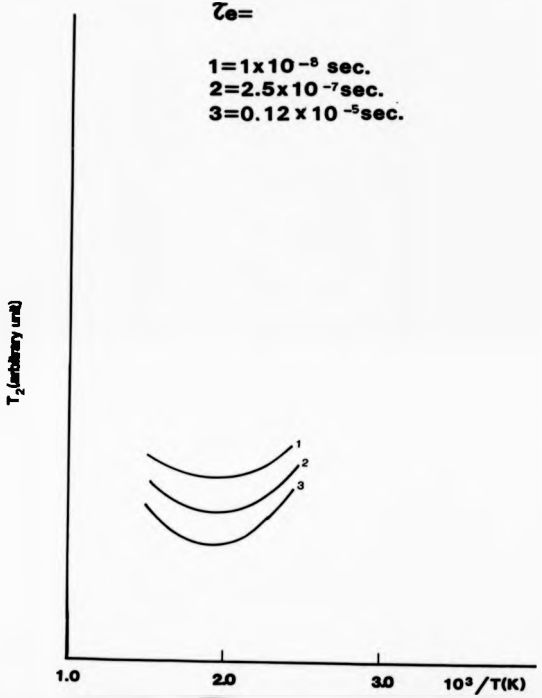

Fig.4.13 T_2 **for different values of the lifetime of the paramagnetic ion.**

sample is estimated to yield about 1.6 x 10^3 ppm. Since the number of paramagnetic ions is very important in accepting the validity of the interaction, some other type of mechanism must be playing a role in this sample and an alternative mechanism will be discussed in the next section.

(ii) The Dipolar Interaction

In order to overcome the defects of postulating the transferred hyperfine interaction as a source of the relaxation process, an alternative interaction is considered. This interaction is the dipole dipole interaction between the resonant lithium nucleus and the impurity moment of Ti^{3+}. Using the rate of the spin lattice relaxation time equation (2.28), which has the form

$$T_1^{-1} = \frac{2}{5} c\hbar^2 \gamma_I^2 \gamma_S^2 S(S+1) \frac{\tau_c}{1+\omega_o^2\tau_c^2} \frac{1}{r^6} \quad (2.28)$$

where c is the impurity concentration, γ_S and γ_I are the impurity and nuclear gyromagnetic ratios respectively, S is the impurity spin and r is the average Li-Li distance. To evaluate the T_1 minimum from equation (2.28) and comparing it with experimentally obtained value, the parameters are chosen according to table (4.5). With these values the minimum relaxation T_1 was obtained as experimentally measured provided the value of the concentration of paramagnetic ions is taken as 2450 ppm. This value was used to scale the value of T_1 obtained from equation (2.28) to those obtained experimentally. It is worth mentioning that constants such as the activation energy and the attempt frequency which contribute to the evaluation of equation (2.28) are taken from the experimental T_1 curve. A fit to T_1 data over the whole temperature range has been obtained using equation (2.28) and is shown in fig. (4.14). Assuming T_1 varies linearly with the concentration of paramagnetic ions, the sample with high purity and which was referred to in the text as the stoichiometric $Li_2Ti_3O_7$ has a

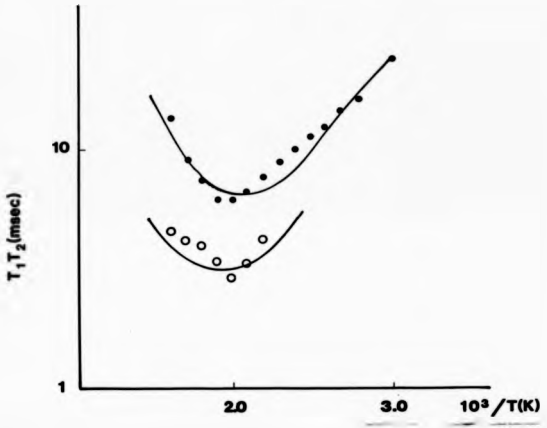

Fig.4.14 The contribution to T_1(•) and T_2(o) due to paramagnetic ions in $Li_2Ti_3O_7$. The solid lines obtained using equation (2.28).

TABLE (4.4)

Activation energy Ea (ev)	0.4
Attempt frequency ν_o $(sec)^{-1}$	10^{10}
Li-Li Average distance r(Å)	2.9
Van Vleck second moment Ω (sec^{-2})	3×10^{-7}

TABLE (4.5)

Nuclear gyromagnetic ratio γ_n oe^{-1} sec^{-1}	1.04×10^4
Impurity gyromagnetic ratio γ_e oe^{-1} sec^{-1}	5.0×10^6
Spin of the impurity (Ti^{3+}) S	$\frac{1}{2}$
Li-Li average distance r Å	2.9
Impurity concentration C PPM	2450

level of paramagnetic ions of 612 ppm which is not surprising since an EPR experiment had shown a small peak in the spectrum.

The dipolar interaction is also responsible for the behaviour of the spin spin relaxation time above 180°C. As indicated frequently in the high temperature region of T_1 and T_2, their ratio equals to 4 was satisfied in few cases such as for Li_5AlO_4 Follstaedt et al (1978) and $LiYZrS_2$ O. Abou et al (1982). For $Li_2Ti_3O_7$ the ratio was found to be about 2.5, hence to fit T_2 data, the values of T_1 obtained through equation (2.28) was divided by the constant 2.5 and is shown in fig. (4.14). At temperatures below 180°C, the interaction is dominated by dipole dipole interaction between the diffusing lithium ions.

4.1.5 Discussion of $Li_2Ti_3O_7$ data

The essence of working on the $Li_2Ti_3O_7$ and on the off stoichiometric sample is to put forward some explanation of the type of relaxation processes taking place in these materials. It is clear from the fitting procedure to two theoretical models, the hyperfine and the dipolar interactions that the agreement between the theory and experimental data is acceptable. The defect in using the transferred hyperfine as a source of relaxation is the unrealistic value for the concentration of paramagnetic ions which was overcome by using the electronic spin-nuclear dipolar interaction as a source of relaxation, producing consistent results by using only constants obtained experimentally.

The measurements also provide an answer to the question of the anomalous value of the attempt frequency, which was found by Huberman et al (1978) to be about 10^7 Hz and led them to suggest that the absolute rate theory is no longer valid in this material. It seems that they developed their theory believing the data measured by them was from intrinsic materials. Two factors were responsible for the anomalous low

prefactor value obtained by the previous authors.

(i) Due to the lack of the frequency dependence of T_1, they used the rigid lattice approximation to get a value for the attempt frequency. This has often resulted in getting a value different from that obtained through the relation $\omega_o\tau_c \sim 1$ at T_1 minimum. For instance in the case of the α-phase of Li_5AlO_4 Follstaadt et al (1978) which satisfied BPP frequency dependence at T_1 minimum, the prefactor was estimated to be 2×10^{12} Hz, while using the rigid lattice approximation, a value of the prefactor was found to be 1.9×10^{10} Hz.

(ii) The use of an activation energy of 0.2ev, which is smaller than the value of 0.4ev obtained from conductivity measurements, will always lead to a lower value of the prefactor. The low value of the activation energy is due to the fact that the sample used by Huberman et al (1978) was not very pure. Using a sample with high purity as in the case of our stoichiometric sample, then a value of the activation energy of 0.4ev from T_2 is obtained. With such a value, Huberman's data would give a value for the attempt frequency of 10^{10}Hz which is three orders of magnitude higher than his stated value.

It seems that our measurements have succeeded in explaining a few points.

(a) The effect of paramagnetic ions dominate T_1 and also T_2 at high temperature even in the cases where the samples are considered nominally pure.

(b) The use of the magnetic tagging technique is also useful in systems with $I > \frac{1}{2}$.

(c) The prefactor obtained from both T_1 minimum and through the rigid lattice limit is about 10^{10} Hz. This value is still considered low compared with the phonon frequency which is in the range of $10^{12} - 10^{13}$

Hz. This low value of the prefactor is not peculiar to $Li_3Ti_3O_7$ but includes several fast ion conductors as explained in Chapter one.

One problem where the theory is not satisfying is the frequency dependence of T_1, where Richards' (1978) theory on paramagnetic impurity and the alternative version of it by O. Abou et al (1982) predicted, as in the case of BPP theory, that $T_1 \propto \omega_o^2$. Unfortunately few data are available in the literature but the work of Follstaedt et al (1978) on $LiAlSiO_4$ or $Li_2Ti_3O_7$ studied by Huberman et al (1978) together with our off stoichiometric $Li_2Ti_3O_7$ all data show no frequency dependence. Other fast ion conductors such as the stoichiometric $Li_2Ti_3O_7$ show that $T_1 \propto \omega_o^{1.8}$ while for Li_5AlO_4, $T_1 \propto \omega^{1.8}$ and for $Li_{12}Mg_2(SiO_4)_4$ (Chapter five) $T_1 \propto \omega^{1.5}$.

4.2.1 Li_2TiO_3

Li_2TiO_3 is a member of the LiTiO system. It crystallizes in a monoclinic structure with lattice parameters a = 5.04Å, b = 8.8 Å and c = 9.72 Å. This structure does not have tunnels as in the case of $Li_2Ti_3O_7$. From structural considerations Li_2TiO_3 was not expected to be a fast ion conductor.

The study was intended to observe motional narrowing which indicates some motion and perhaps higher conductivity. The increase of conductivity could be the result of transformation from an insulating to a conducting state at some higher temperature. Also measuring T_1 and T_2 yield some dynamical parameters such as the activation energy and the attempt frequency which will help any future work concerning this material.

The investigation was concerned with measuring the spin lattice and spin spin relaxation times at two frequencies of 12.3 and 7.5 MHz, in the temperature range from 250°C to 730°C.Fig. (4.15) shows T_1 and T_2 at the two frequencies versus 1/T. The curves indicate that

(i) T_1 is frequency independent which could be due to the existence of paramagnetic ions especially as indicated by Johnson et al (1964) that in LiTiO group the electronic and ionic conductivities vary from one solid to another. If the transference number is measured in Li_2TiO_3 it might show that it is a mixed conductor. The lack of frequency dependence would not allow an estimate of the attempt frequency from T_1 minimum, hence this value was obtained from T_2. Below the minimum, T_1 increases with decreasing temperature, yielding an activation energy of about 0.45 eV.

(ii) Motional narrowing was observed between 370°C and 500°C yielding activation energy of 0.47 eV, similar to that obtained from T_1 measurements indicating that the mechanism responsible for T_1 and T_2 relaxations is the same. In this temperature range one expects some

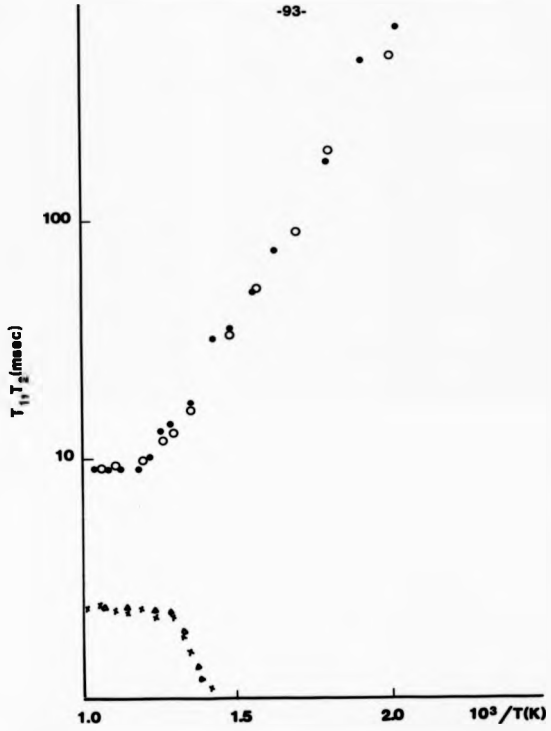

Fig.4.15 T_1 for ^7Li in Li_2TiO_3 at 12.3MHz(•) and 7.5MHz(○). T_2 data obtained at 12.3MHz(×) and 7.5MHz(△).

conduction is taking place. To get an estimate of the correlation time for motion, the data yields a value of 4×10^{-4} sec at a temperature of 400°C, while in the case of $Li_2Ti_3O_7$, the room temperature value for the correlation time is 5×10^{-4} sec. This comparison supports the notion that Li_2TiO_3 is not a fast ion conductor.

(iii) At temperatures above 500°C both T_1 and T_2 show a temperatures independent behaviour, since the ratio T_1/T_2 is about 4 in this temperature range, one could assume that the relaxation processes are due to paramagnetic ions.

(iv) The onset of motional narrowing was considered at T = 370°C and hence a value of 10^7 Hz was obtained for the attempt frequency.

CHAPTER FIVE

THE LISICON GROUP

5.1 Introduction to the Lisicon System

Hong (1978) discovered a group of lithium ion conductors, with the formula type $Li_{16-2x}D_x(TO_4)$, where D is the divalent cation (Mg^{2+} or Zn^{2+}), T is the tetravalent cation (Si^{4+} or Ge^{4+}) and $0 < x < 4$. One of these materials $Li_{14}Zn(GeO_4)_4$ which he called Lisicon (Lithium superionic conductor), has an ionic conductivity of 0.125 $(\Omega cm)^{-1}$ at a temperature of 300°C. The best oxides reported previously, such as Li β-alumina, $Li_{3.75}Si_{0.75}P_{0.25}O_4$ and $Li_{3.5}Si_{0.5}P_{0.5}O_4$ have conductivities at 300°C of 9 x 10^{-3}, 1 x 10^{-2} and 3.2 x 10^{-2} $(\Omega\ cm)^{-1}$ respectively. Therefore $Li_{14}Zn(GeO_4)_4$ has an ionic conductivity higher than any lithium ion conductor reported previously, fig. (5.1).

Lisicon crystallizes in a space group pnma with cell parameters as a = 10.8Å, b = 6.25Å, C = 5.14Å and z = 1. The lithium ions are distributed among four sites; four ions occupy 4c site designated Lz(1) and seven ions occupy 8d sites designated Lz(2), the designation Lz indicates that the site is occupied both by lithium and zinc ions. The eleven lithium ions form a part of the rigid three dimensional network represented by $[Li_{11}Zn(GeO_4)]^{3-}$ with the remaining three Li ions in interstitial sites and the migration of lithium ions between these sites cause the high lithium conductivity, fig. (5.2).

The high ionic conductivity of these materials in the temperature range 300°C to 400°C, shown in fig. (5.3), encouraged many investigators to use different experimental techniques such as x-rays, conductivity and DTA to study their properties. At the beginning of this work there was no

nuclear magnetic resonance study of these materials available in the literature. This encouraged the idea of investigating some of these compounds through the measurements of the spin-lattice and spin-spin relaxation times and to correlate the NMR data with those obtained from the conductivity measurements to understand the conduction processes in these materials.

The work concentrated on studying two compounds, the choice is based on selecting materials with high ionic conductivity and on the availability of the starting materials locally. Therefore $Li_{12}Zn_2(SiO_4)_4$ and $Li_{12}Mg_2(SiO_4)_4$ were prepared using the materials lithium carbonate, zinc oxide, magnesium oxide and silicon oxide. These compounds have ionic conductivities of 6.2×10^{-3} and 6.9×10^{-4} $(\Omega cm)^{-1}$ respectively at a temperature of 300°C according to fig. (5.3).

One of the early studies of the Lisicon $Li_{14}Zn(GeO_4)_4$ through conductivity measurements was performed by Mazumdar et al (1983) whose sample was prepared as described by Hong (1978). The measurements were carried out using the complex impedance method in a frequency range of 70 Hz to 100 kHZ and in the temperature range of 35 to 350°C. The data collected are used to plot log σ T versus 1/T, where σ is the ionic conductivity and T is the absolute temperature and is shown in fig. (5.4). The value obtained for the conductivity at temperature of 300°C and the value of the activation energy yielded from the curve were different from those obtained by Hong (1978). A literature survey revealed the conductivity and activation energy reported for $Li_{14}Zn(GeO_4)_4$ by different workers following Hong's method of preparation, vary widely as shown in table (5.1). These discrepancies could be attributed to the use of different electrode materials, existence of impurities in the starting materials and possibly different pellet pressures, by different workers.

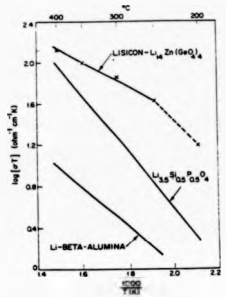

Fig.5.1 Ionic conductivity of some lithium ion conductors (Hong 1978).

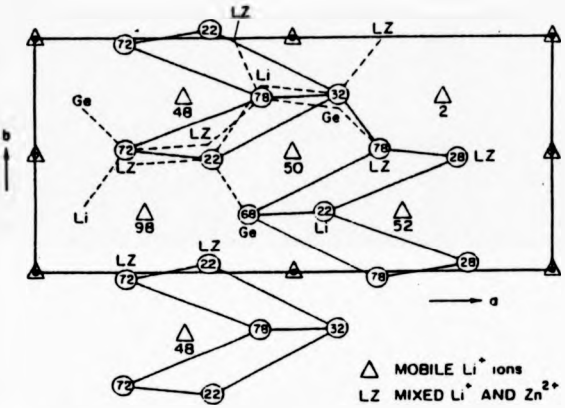

Fig.5.2 Projection of the $Li_{14}Zn(GeO_4)_4$ structure on the a–b plane (Hong 1978).

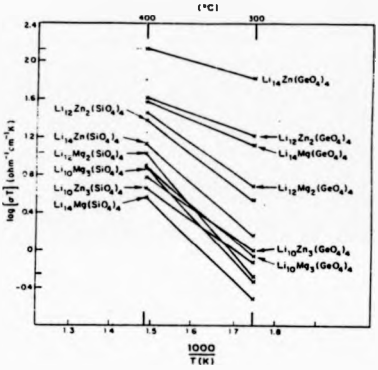

Fig.5.3 Product of conductivity and temperature as a function of inverse temperature for $Li_{16-2x}D_x(TO_4)_4$ samples (Hong 1978).

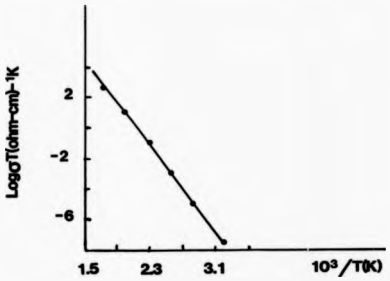

Fig.5.4 Ionic conductivity as a function of inverse temperature for $Li_{14}Zn(GeO_4)_4$(Mazumdar et al 1983)

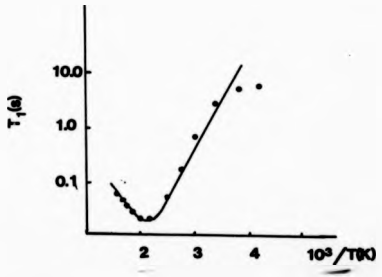

Fig.5.5 T_1 for ^7Li in $Li_{14}Zn(GeO_4)_4$ at 40MHz (Bose et al 1986).

TABLE (5.1)

The conductivity σ of $Li_{14}Zn(GeO_4)_4$ reported by different workers

Conductivity at 300°C $(\Omega\ cm)^{-1}$	ΔE ev	Temp. range °C	Reference
1.3×10^{-1}	0.24	(300 - 400)	Hong (1978)
1.0×10^{-1}	0.89	(20 - 300)	Bayard (1979)
1.0×10^{-1}	0.80	(20 - 450)	Schoonman (1979)
1.7×10^{-3}	0.56	(50 - 300)	Alpen (1978)
2.4×10^{-3}	0.60	(30 - 300)	Mazumdar (1983)

These variables play a leading role in determining the value of the conductivity. These variations in the reported values of the conductivity and the activation energy triggered Bose et al (1986) to investigate this compound microscopically through nmr. The work concentrated on studying the dynamics of Lisicon through measurements of the spin lattice relaxation time in the temperature range -70 to 400°C and at a frequency of 40 MHz.

The T_1 data against 1/T is plotted in fig. (5.5), showing a minimum at temperature of 203°C. Below the minimum T_1 increases exponentially with the decrease of temperature and the slope yielded an activation energy of 0.37 eV. compared with that of 0.25 eV. obtained from the conductivity measurement. With these data the value of the attempt frequency from the relation $\omega_o\tau_c \sim 1$ at the minimum was found to be 2.13 x 10^{12} sec^{-1} and the data was fitted to a BPP type of relaxation. At high temperature the relaxation was thought to be dominated by quadrupolar fluctuation due to lithium motion. Rong (1981) detected a quadrupolar satellite in lisicon in the temperature range 180°C to 250°C and reported a value of 38 kHz. for quadrupolar coupling constant. Bose et al (1986) used this value to calculate T_1 minimum and found close agreement.

This NMR investigation was the first attempt to study any of this group of conductors. It neither investigated the effect of frequency on T_1 nor measured the spin-spin relaxation time T_2. The task of the present study is to elaborate on this investigation to provide more information so as to be able to understand the mechanism of the conduction processes in these solids.

5.2 Relaxation Times Studies

The measurements consisted of measuring the spin lattice relaxation time T_1 in the temperature range from 150°C to 400°C at two Larmor

frequencies of 12.3 and 7.5 MHz. The method used in measuring T_1 is the inversion recovery (180-τ-90) pulse sequence. The spin spin relaxation time T_2 was measured for both compounds in the same temperature range as T_1 and at a frequency of 12.3 MHz. The measurements were performed using Hahn's spin echo (90-τ-180) pulse sequence.

Fig. (5.6 and 5.7) show the measured T_1 versus 1/T for $Li_{12}Mg_2(SiO_4)_4$ and $Li_{12}Zn_2(SiO_4)_4$ at different frequencies. It is clear from the curves that as the temperature is lowered the relaxation time T_1 decreases until the stage where τ_c, the lithium diffusion correlation time, becomes long enough to be comparable with the Larmor period. The spin lattice relaxation time passes through a minimum and then increases with the decrease of temperature. The minima occur at temperatures of about 332°C and 297°C for $Li_{12}Mg_2(SiO_4)_4$ and $Li_{12}Zn_2(SiO_4)_4$ respectively. At the T_1 minimum where $\omega_o \sim \tau_c^{-1}$, an attempt frequency can be found once the activation energy is obtained from the low temperature part of the T_1 curve. These experimental parameters are tabulated in table (5.2). The activation energies from above and below the minimum are the same, an indication that the relaxation processes are dominated by the same mechanism.

In $Li_{12}Mg_2(SiO_4)_4$, T_1 was measured at two frequencies 12.3 and 7.5 MHz, as shown in fig. (5.6). The low frequency values of T_1 are shorter than those at the higher frequency showing a frequency dependent process. The dependence of T_1 is $\omega_o^{1.5}$ instead of ω_o^2 as expected for normal BPP behaviour. The minima of T_1 for both frequencies occur at temperatures of about 332°C and 308°C indicating $T_{1min.} \propto \omega_o^{1.0}$ as predicted by BPP, while at high temperature T_1 is shown to be independent of frequency.

Figs. (5.6 and 5.7) also show the data for the spin spin relaxation time T_2 for both compounds versus 1/T plot. The trend for both curves is

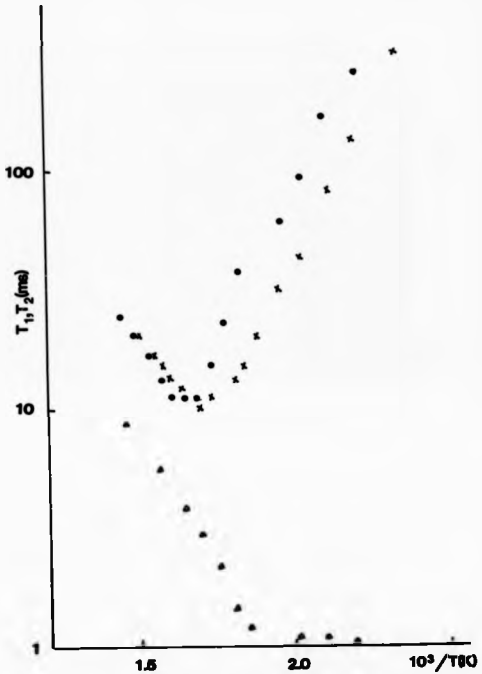

Fig.5.6 T_1 and T_2 as a function of temperature for ^7Li in $Li_{12}Mg_2(SiO_4)_4$. T_1 data was obtained at 12.3MHz(•), 7.5MHz(×) and T_2 at 12.3MHz(Δ).

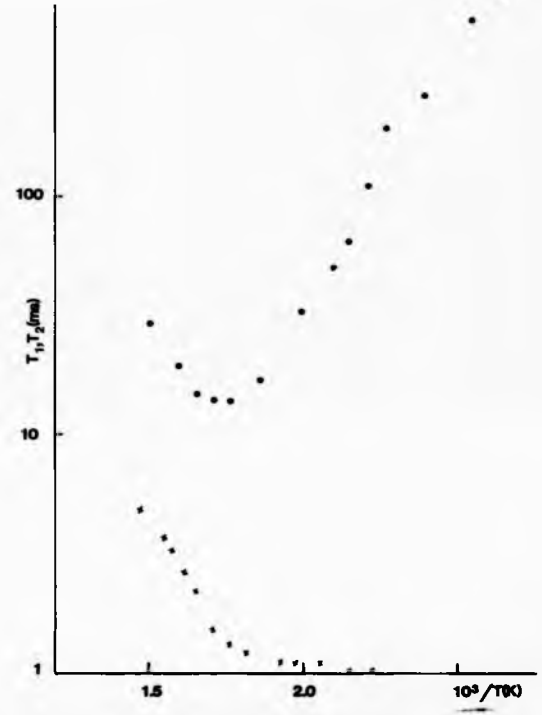

Fig.5.7 T_1 and T_2 as a function of temperature for ^{7}Li in $Li_{12}Zn_2(SiO_4)4$. T_1 data was obtained at 12.3MHz(•) and T_2 at 12.3 MHz(×).

TABLE (5.2)

Sample	E_{nmr}(ev)	ν_o(sec.-1)
$Li_{12}Mg_2(SiO_4)_4$	0.5	1×10^{12}
	(T_1,T_2)	(T_1)
		1×10^{8}
		(T_2)
$Li_{12}Zn_2(SiO_4)_4$	0.43	0.47×10^{12}
	(T_1,T_2)	(T_1)
		3×10^{7}
		(T_2)

that in the temperature range from 200°C to 400°C, T_2 increases with the increase of temperature indicating a motional narrowing region and the curves yield activation energies close to those obtained from T_1 measurements. At T < 200°C, T_2 approaches a constant value which corresponds to the rigid lattice case. In this region one expects the linewidth to be proportional to square root of the Van Vleck second moment. Experimentally the linewidth was found to be 10^3 sec.$^{-1}$ while the calculated second moment gives a value of 2.8×10^3 sec.$^{-1}$, showing a reasonable agreement. At the onset of motional narrowing $T_2 \sim \tau_c$ yielding values for the attempt frequencies much smaller than the ones obtained through T_{1min} as shown in table (5.2). T_1 and T_2 at high temperature for both solids should be the same, but it was found that their ratio approaches a value consistent with relaxation by paramagnetic centres.

5.3 Data analysis for the Lisicon Group

In order to identify the type of interaction playing a role in these materials, the magnitude of T_1 at the minimum using the dipole dipole interaction between the diffusing lithium ions is examined. The strength of the interaction is given by Van Vleck's second moment Ω as

$$T_{1min}^{-1} = \Omega \tau_c$$

Using the NMR data taken at a frequency of 12.3 MHz. and the calculated value for the second moment as 8.18×10^6 sec.$^{-2}$, then equation (2.18) gives

$$T_{1min} = 9.4 \text{ sec.},$$

while experimentally $T_{1min.} = 11 \times 10^{-3}$ sec., about three orders of magnitude smaller than the calculated value. This should exclude the possibility that the dipolar interaction between the lithium ions plays an important role as a source of relaxation.

For the Lisicon system where the diffusing ion is lithium which has a spin of 3/2, one might expect some influence from the quadrupolar relaxation hence one needs to find the quadrupolar coupling constant. Rong (1981) and later Bose et al (1986) found that for $Li_{14}Zn(GeO_4)_4$, the constant has a value of 38 kHz, hence this value is used to calculate T_{1min} as

$$(T_{1min})_Q^{-1} = \left(\frac{e^2qQ}{\hbar}\right)^2 \tau_c, \qquad (2.24)$$

where $\frac{e^2qQ}{\hbar}$ is the quadrupolar coupling constant. Equation (2.24) gives,

$$(T_{1min})_Q = 48 \text{msec.},$$

This value is not far from the experimental value but for quadrupolar interaction to be responsible for relaxation, it is required that the ratio T_1/T_2 of the high temperature part should be unity, a criterion not fulfilled by $Li_{12}Mg_2(SiO_4)_4$. The data of fig. (5.6) gives the ratio as about 3, which excludes the quadrupolar interaction as a source of relaxation.

The approximate value of T_1/T_2 close to 4 indicates that paramagnetic ions are playing a role in the relaxation process. Examining the supplier's specifications of the different constituents of these samples revealed the existence of Fe^{3+} in both $Li_{12}Mg_2(SiO_4)_4$ and $Li_{12}Zn_2(SiO_4)_4$. It is possible that Fe^{3+} ions have taken the place of some of Mg^{2+} or Zn^{2+} ions and in order for charge neutrality one expects for every two Mg^{2+} or Zn^{2+} ions to be replaced by Fe^{3+} and a vacancy for lithium. The mechanism responsible for the relaxation was thought to be the dipolar interaction between the magnetic moment of the diffusing lithium ion and the electronic magnetic moment of Fe^{3+}. This mechanism was used before in the case of $Li_2Ti_3O_7$ in Chapter IV. The relaxation rates in this formalism were given by Abragam (1961) and were discussed in Chapter Two. The spin lattice relaxation rate is given by

$$T_1^{-1} = \frac{2}{5} c\hbar^2 \gamma_I^2 \gamma_S^2 S(S+1) \frac{\tau_c}{1+\omega_o^2\tau_c^2} \sum_n \frac{1}{r_n^6} \qquad (2.28)$$

where the symbols of equation (2.28) were explained previously. With the use of the parameters given in table (5.3) the value of the T_1 minimum obtained experimentally could be reproduced from equation (2.28) provided the concentration of paramagnetic ions of Fe^{3+} are taken as 0.00018 and 0.00025 in the samples $Li_{12}Mg_2(SiO_4)_4$ and $Li_{12}Zn_2(SiO_4)_4$ respectively. The concentration of paramagnetic ions is used as a scaling factor to ensure the correspondence between T_1 data obtained experimentally and those calculated from equation (2.28). The value of the spin lattice relaxation times for both $Li_{12}Mg_2(SiO_4)_4$ and $Li_{12}Zn_2(SiO_4)_4$ at different frequencies are shown in figs. (5.8, 5.9 and 5.10), the solid lines are the theoretical fits using the data given in table (5.3). The values of impurity concentration used in the fitting procedure is about one order of magnitude higher than the specified value given by the supplier. Another approximation used in equation (2.28) is the substitution of r which is the distance between the position of the impurity Fe^{3+} and the position of the diffusing lithium ion, by the average distance between lithium ions obtained from the structure.

In order to fit T_2 to a theoretical model the relation obtained by Fedder (1976) is used which assumes that above T_1 minimum, the ratio of $T_1/T_2 = (I + \frac{1}{2})^2$ should be 4 in the case of lithium, provided the relaxation processes are caused by paramagnetic ions. Experimental data measured at a frequency of 12.3 MHz revealed that this ratio is 3 and 4 for $Li_{12}Mg_2(SiO_4)_4$ and $Li_{12}Zn_2(SiO_4)_4$ respectively. The ratio factor obtained experimentally was used to scale the value of T_1 obtained through equation (2.28). The result of this procedure is a solid line fitting the experimental data as shown in fig. (5.9 and 5.10).

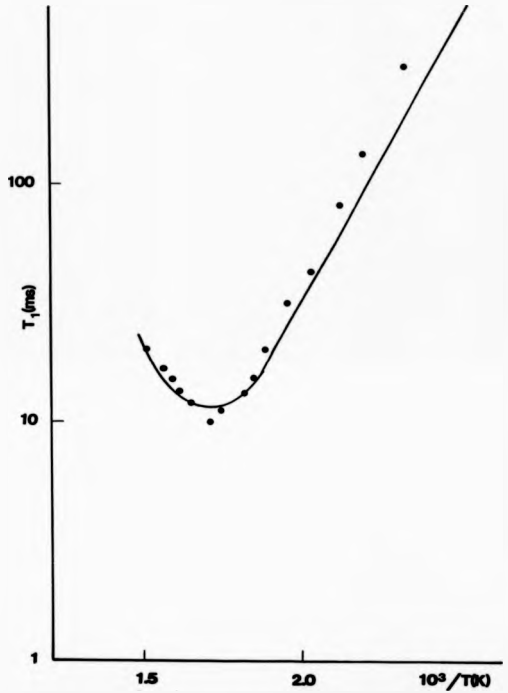

Fig.5.8 T_1(•) data for $Li_{12}Mg_2(SiO_4)_4$ at 7.5MHz. The curve is a theoretical fit with parameters given in the text.

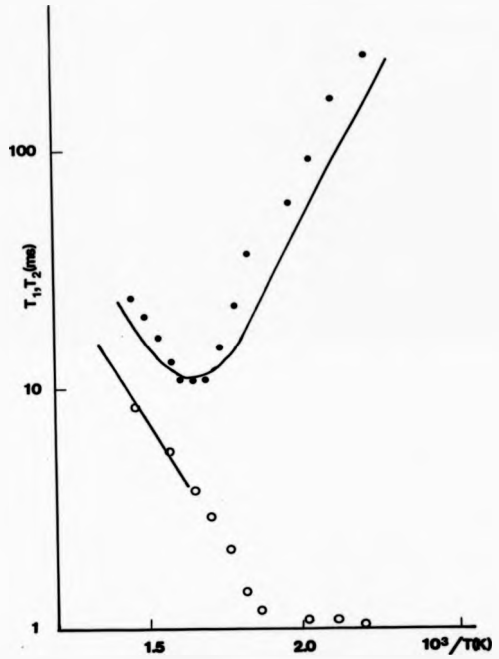

Fig.5.9 T_1(•), T_2(o) data for $Li_{12}Mg_2(SiO_4)_4$ at 12.3MHz. The curves are theoretical with parameters given in the text.

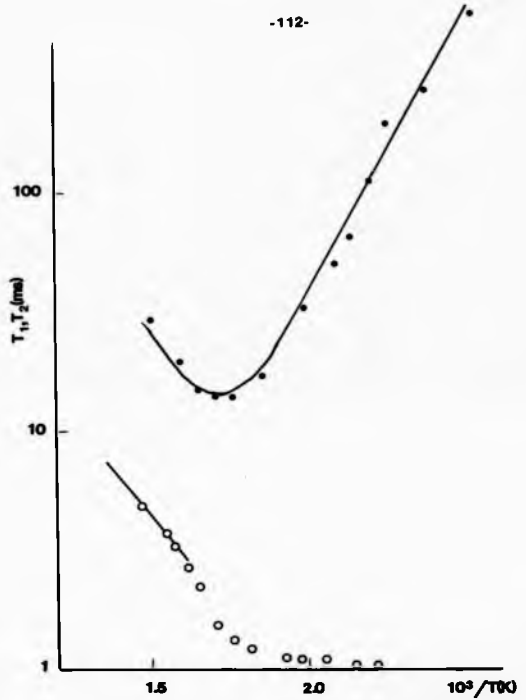

Fig.5.10 T_1(•), T_2(○) data for $Li_{12}Zn_2(SiO_4)_4$ at 12.3MHz. The curves are theoretical with parameters given in the text.

TABLE (5.3)

Constants used in equation (2.28)

Nuclear gyromagnetic ratio γ_I	1.04×10^4 oe^{-1} $sec.^{-1}$
Impurity gyromagnetic radio γ_s	1.76×10^7 oe^{-1} $sec.^{-1}$
Spin of the impurity S	5/2
Li-Li average distance r	3.6Å
Impurity concentration in $Li_{12}Mg_2(SiO_4)_4$	0.00018
Impurity concentration in $Li_{12}Zn_2(SiO_4)_4$	0.00025

5.4 Discussion of the Experimental Data

The study carried out on $Li_{12}Mg_2(SiO_4)_4$ and $Li_{12}Zn_2(SiO_4)_4$ and the deduction of the mechanism responsible for the relaxation processes, results in data which will enrich further investigations on these materials through other experimental techniques. The conductivity measurements of these materials which is shown in fig. (5.3) allow the classification of this group as belonging to class III of the fast ion conductors. The data of T_1 and T_2 seem to reflect some of the anomalies encountered in this group of materials. One deviation is the weak dependence of the spin lattice relaxation time on Larmor frequency as

$$T_1 \propto \omega_o^{1.5},$$

instead of $T_1 \propto \omega_o^{2.0}$ for the case of BPP theory. This result reflects a property shared by that class of fast ion conductors. At the minimum, T_1 is found to vary with the frequency as

$$T_{1min.} \propto \omega_o^{1.0}$$

agreeing with BPP theory. The relaxation rates T_1 and T_2 have shown thermally activated lithium motion yielding activation energies of 0.5 and .43 eV from the low temperature part of T_1 and the motional narrowing region of T_2 for both compounds. Also at the T_1 minimum attempt frequencies of 10^{12} sec^{-1} and 5×10^{11} sec^{-1} for both samples were obtained. They are close to the phonon frequency, hence there is no prefactor anomaly as observed in several other ionic conductors.

CHAPTER SIX

CONCLUSIONS

One conclusion that can be drawn from the experimental data obtained from fast ion conductors is if one wants to study the intrinsic properties of a material via NMR, it is essential to make sure the sample is free of paramagnetic ions, since it has been shown that even a few ppm have a large effect on the relaxation rates. Some anomalies in the relaxation behaviour which suggest that the relaxation rates may be influenced by paramagnetic ions are:

(i) An extra peak in the spin-spin relaxation time versus inverse of temperature curve.

(ii) The spin lattice relaxation time below the minimum shows a T_1 dependence on ω_o of ω_o^{α} where $\alpha < 2$.

(iii) A low value for the attempt frequency.

Therefore if the material under investigation shows some of these anomalies, it is advisable to check the level of paramagnetic ions before one tries to interpret the data assuming the sample is nominally pure.

In $Li_2Ti_3O_7$ the variation of T_1 below the minimum with Larmor frequency should be tested further. In the stoichiometric sample T_1 varies with $\omega_o^{1.0}$ but for the off stoichiometric sample T_1 is independent of frequency, which might suggest that the level of paramagnetic ions is playing some role. Hence one would suggest a future investigation varying the level of the lithium ions introduced to produce samples with different impurity concentrations. The study of the relaxation rates as a function of temperature for these samples would reveal how the relaxation rates depend on the impurity level. Also performing the measurements at

different frequencies might show the dependence of the spin lattice relaxation rate on frequency. In $Li_2Ti_3O_7$ it was thought that the introduction of Li ions into the stoichiometric $Li_2Ti_3O_7$ results in converting Ti^{4+} into Ti^{3+} which is a paramagnetic ion, affecting the relaxation processes. It would be interesting to introduce some TiO_2 into the stoichiometric $Li_2Ti_3O_7$ to see its effects on the relaxation rates.

The question concerning the low value of the attempt frequency could be the product of the effect of the paramagnetic ions and the way it is deduced. The data for the off stoichiometric $Li_2Ti_3O_7$ and for lisicon group studied in this thesis, always gave a higher value of the attempt frequency obtained from the T_1 minimum than that obtained from T_2 at the onset of motional narrowing. The discrepancies between the two values are as high as few orders of magnitude. This is confusing especially when one tries to compare the value obtained by NMR with that obtained through for example, the a.c. conductivity.

In the lisicon group it would be interesting to have a thorough investigation of $Li_{14}Zn(GeO_4)$ through measurements of T_1 and T_2 and compare the results with the already existing data from other experimental techniques. This compound is the only one in the group of lisicon to be investigated by a few researchers, therefore integrating their data with the NMR results, would benefit the study of fast ion conductors. In the case of the other compounds of the lisicon group studied here, it would be a worthwhile exercise to study their relaxation rates, but one should start with very pure materials so that a comparison can be achieved.

REFERENCES

Abragam, M, Principle of Nuclear Magnetism, Oxford, New York (1961)

Alpen, U.V. and M.F. Bell, in Fast Ion Transport in Solids, p.463, North Holland, New York (1979)

Alpen, U.V., H. Schulz, G.H. Talat and H. Bohm, Solid State Commun. 23, 911 (1977)

Azaroff, L., Elements of X-ray Crystallography (McGraw-Hill, Inc. (1968))

Bayard, M.L. in Fast Ion Transport in Solids, p.479, North Holland, New York (1979)

Bjorkstam, J.L. and M. Villa, Magn. Reson. Rev. 6, 2 (1980)

Bloembergen, N., E.M. Purcell and R.V Pound, Phys. Rev. 73, 679 (1948)

Bose, M., A. Basu and D. Torgenson in Solid State Ionic 18, 539 (1986)

Boukamp, B.A. and R.A. Huggins, Phys. Lett. 58A, 231 (1976)

Boyce, J.B. and B.A. Huberman, Phys. Reports 51, 139 (1979)

Boyce, J.B., J.C. Mikkelsen and B.A. Huberman, Solid State Commun. 29, 507 (1979)

Boyce, J.B. and J.C. Mikkelsen, Solid State Commun. 31, 741 (1979)

Chandra, S., Superionic Solids, North-Holland, Amsterdam (1981)

Clark, W.G., Rev. Sci. Inst. 35, 316 (1964)

Dreyfus, R.W. and A.S. Nowick, Phys. Rev. 126, 1367 (1962)

Dupree, R., J.R. Howells, A. Hooper and F.W. Poulsen in Solid State Ionics, Eds. M. Kleitz, B. Sapoval and Y. Chabre, North-Holland, Amsterdam (1983)

Fedders, P.A., Phys. Rev. B 13, 2768 (1976)

Follstaedt, D.M. and P.M. Richards, Phys. Rev. Lett. 37, 1571 (1976)

Follstaedt, D.M. and R.M. Biefeld, Phys. Rev. B 18, 5928 (1978)

Geller, S., Science 176, 1016 (1972)

Hahn, E.L., Phys. Rev., 80, 580 (1950)

Halstead, T.K., W.U. Benesh, R.D. Gulliver and R.A. Huggins, J. Chem. Phys. 58, 3530 (1973)

Hoggs, R.D., S.P. Vernon and V. Jaccarino, Phys. Rev. Lett. 39, 481 (1977)

Hong, H. Y-P., Mater. Res. Bull., 13, 117 (1978)

Hu, Y.W., I.D. Raistrick and R.A. Huggins, Mater. Res. Bull., 11, 1227 (1976)

Huberman, B.A. and J.B. Boyce, Solid State Commun. 25, 759 (1978)

Huggins, R.A., Stanford University Tech. Rep. AD 773972 (1973)

Huggins, R.A., Electrochim. Acta 22, 773 (1977)

Izquierdo, G. and A. West, Solid State Commun. 15, 1655 (1980)

Johnson, O.W., Phys. Rev. A 136, 284 (1964)

Kennedy, J.H., in Physics of Solid Electrolytes, Ed. S. Geller (Springer-Verlag, New York 1977)

Kubo, R. and K. Tomita, J. Phys. Soc. Jpn. 9, 888 (1954)

Kvist, A. and A. Lunden, Z. Naturf. 20a, 235 (1965)

Lidiard, A.B., in Handbuch der Physik, Ed. S. Flugge, 20, p.246 (Springer-Verlag, Berlin 1957)

Lowe, I.J. and C.E. Tarr, J. Sci. Inst. 2, 320 (1968)

Lundberg, M. and S. Andersson, Acta. Chem. Scand. 18, 817 (1964)

Mazumdar, D., D.N. Bose, N.L. Mukherjee, A. Basu and M. Bose, Mater. Res. Bull., 18, 79 (1983)

Morosin, B. and J.C. Mikkelsen, Acta. Cryst. B 35, 798 (1979)

O.Abou, G., S. Clough and L. Trichet, J. Phys. C: Solid State Physics 15, 5113 (1982)

Raistrick, I.D., C. Ho and R.A. Huggins, Mater. Res. Bull. 11, 953 (1976)

Reau, J.M., G. Magniez, L. Rabardel, J.P. Chaminad and M. Pouchard, Mater. Res. Bull. 11, 867 (1976)

Rice, M.J. and W.L. Roth, J. Solid State Chem. 4, 294 (1972)

Richards, P.M., Solid State Commun. 25, 1019 (1978)

Richards, P.M., Phys. Rev. B 18, 6358 (1978)

Richards, P.M., in Topics in Current Physics, Physics of Superionic Conductors, Ed. M.B. Salamon (Springer, Berlin 1979)

Rong Li-Zi, Xue Rong-Jian and Chen Li-quan, Acta Physica Sinica 30 No. 10, 1389 (1981)

Schlaikyer, C.R. and C.C. Liang, in Fast Ion Transport in Solids, Ed. W. Van Gool, p.685 (North-Holland, Amsterdam, 1973)

Schoonman, J., J.G. Kamphorst and E.E. Hellstrom, in Materials for Advanced Batteries, p. 247 (Plenum Press, New York 1979)

Shahi, K. and S. Chandra, J. Phys. C 8, 2255 (1975)

Shannon, R.D., B.E. Taylor, A.D. English and T. Berzins, Electrochim. Acta. 22, 783 (1977)

Silbernagel, B.G., F.R. Gamble, Phys. Rev. Lett. 32, 1436 (1974)

Strock, L.W., Z. Phys. Chem. B 25, 411 (1934)

Takahashi, T. and Denki Kagaku, 38, 360 (1970)

Takahashi, T., J. Appl. Electrochem. 3, 79)1973)

Takeshi, A. and S. Kawai, Solid State Commun. 36, 891 (1980)

Van Gool, W., in Fast Ion Transport in Solids, Ed. Van Gool, W. (North-Holland, Amsterdam 1973)

Van Vleck, J.H., Phys. Rev. 74, 1168 (1948)

Walstedt, R.E., Phys. Rev. Lett. 19, 146 (1967)

Weaver, H.T. and R.M. Biefeld, Solid State Commun. 18, 39 (1976)

West, A.R., J. Appl. Electrochim. 3, 327 (1973)

Whittingham, M.S. and B.G. Silbernagel, in Solid Electrolytes: General Principles, Characterization, Materials, Applications, Ed. P. Hagenmuller, W. Van Gool (Academic Press, New York 1977)

Wiedersich, H. and S. Geller, in The Chemistry of Extended Defects in Non-Metallic Solids, Eds. L. Eyring and M. O'Keeffe, p. 629 (North-Holland, Amsterdam 1970)

Yao, Y.F.Y. and J.T. Kummer, J. Inorg. Nucl. Chem. 29, 2453 (1967)